© 2019. Published by The Company of Biologists Ltd | Journal of Experimental Biology (2019) 222, jeb203620. doi:10.1242/jeb.203620

RESEARCH ARTICLE

Histone deacetylase activity is required for *Botrylloides leachii* whole-body regeneration

Lisa Zondag, Rebecca M. Clarke and Megan J. Wilson*

ABSTRACT

The colonial tunicate *Botrylloides leachii* is exceptional at regenerating from a piece of vascular tunic after loss of all adults from the colony. Previous transcriptome analyses indicate a brief period of healing before regeneration of a new adult (zooid) in as little as 8–10 days. However, there is little understanding of how the resulting changes to gene expression, required to drive regeneration, are initiated and how the overall process is regulated. Rapid changes to transcription often occur in response to chromatin changes, mediated by histone modifications such as histone acetylation. Here, we investigated a group of key epigenetic modifiers, histone deacetylases (HDAC), which are known to play an important role in many biological processes such as development, healing and regeneration. Through our transcriptome data, we identified and quantified the expression levels of HDAC and histone acetyltransferase enzymes during whole-body regeneration (WBR). To determine whether HDAC activity is required for WBR, we inhibited its action using valproic acid and trichostatin A. HDAC inhibition prevented the final morphological changes normally associated with WBR and resulted in aberrant gene expression. *Botrylloides leachii* genes including *Slit2*, *TGF-β*, *Piwi* and *Fzd4* all showed altered mRNA levels upon HDAC inhibition in comparison with the control samples. Additionally, atypical expression of *Bl_Piwi* was found in immunocytes upon HDAC inhibition. Together, these results show that HDAC function, specifically HDAC I/IIa class enzymes, are vital for *B. leachii* to undergo WBR successfully.

KEY WORDS: Epigenetics, Colonial tunicate, Ascidian, Histone modification

INTRODUCTION

Botrylloides leachii whole-body regeneration (WBR) requires a series of rapid molecular and cellular responses as a consequence of loss of all adults (termed zooids). Regeneration of a new zooid occurs in as little as 8–10 days from a vascular fragment (Rinkevich et al., 1995). RNA-sequencing (RNA-seq) followed by differential gene expression analysis between early and late regeneration stages revealed novel information on transcriptional changes during WBR (Zondag et al., 2016). The expression of genes, with known roles in wound healing, cellular organisation and developmental pathways such as transforming growth factor β (TGF-β) and Notch signalling, all changed significantly over the 8 day WBR period (Zondag et al., 2016).

Developmental Biology and Genomics Laboratory, Department of Anatomy, Otago School of Medical Sciences, University of Otago, P.O. Box 56, Dunedin 9054, New Zealand.

*Author for correspondence (meganj.wilson@otago.ac.nz)

M.J.W., 0000-0003-3425-5071

Received 18 March 2019; Accepted 24 June 2019

We predict that the immediate changes to transcription required for *B. leachii* WBR requires an epigenetic mechanism. Modifications to histone proteins, which make up the nucleosome complex, along with chemical additions directly to the DNA such as methylation at CpG sites, represent key mechanisms of gene regulation (Gan et al., 2007; Jopling et al., 2011). These epigenetic modifications function by inducing changes in chromatin structure, either by permitting or restricting DNA accessibility or through the recruitment of DNA-binding proteins (Bannister and Kouzarides, 2011).

The chemical modification of histone proteins is a dynamic process requiring enzymes to add and remove 'marks' to specific amino acids at the N-terminus of histone proteins. Two well-studied groups of enzymes that regulate acetylation of histone proteins are histone acetyltransferases (HAT) and histone deacetylases (HDAC). Different classes of HAT enzymes transfer an acetyl group onto specific lysine residues located within the histone(s) protein target (Lee and Workman, 2007). Generally, HATs promote transcriptional activation through the creation of binding sites for chromatin remodelling complexes to bind and open up the chromatin (Marmorstein and Roth, 2001). HDACs are thought to oppose HAT activity, repressing transcription by removing acetyl groups from histone tails, which causes the chromatin to move towards a heterochromatic state (Gregoretti et al., 2004; Murakami, 2013). Condensing of the DNA around tightly packed nucleosomes prevents transcription factors from accessing transcriptional start sites, repressing local transcription (Ke et al., 2012). Thus, HATs and HDACs are involved in regulating transcription of genes and, consequently, the regulation of many processes including cell proliferation, apoptosis and cell differentiation (Ke et al., 2012).

Cellular reprogramming and re-establishment of lost cell types is a critical process during regeneration, and consequently, HDAC activity is required for successful regeneration in some vertebrates (Huang et al., 2013; Taylor and Beck, 2012; Tseng et al., 2011) and planarians (Eisenhoffer et al., 2008; Reddien et al., 2005; Robb and Sanchez Alvarado, 2014). HDAC inhibition (HDACi) during *Xenopus* tail regeneration by trichostatin A (TSA) and valproic acid (VPA) halts regeneration (Taylor and Beck, 2012; Tseng et al., 2011). In mammalian models, VPA treatment also inhibits the regenerative response. For example, mice exposed to HDAC inhibitors have a reduced ability to regenerate their liver following resection (Huang et al., 2013; Ke et al., 2012). Further studies found that genome-wide acetylation changes following HDACi paralleled changes in gene expression, with some genes normally induced upon initiation of liver regeneration showing reduced expression with HDACi, and genes normally suppressed during liver regeneration having increased expression following HDACi (Huang et al., 2014).

Fewer studies have analysed the specific role of HAT proteins in regards to regeneration. Shibuya et al. (2015) demonstrated that regeneration was still possible in the stolidobranchian tunicate species *Polyandrocarpa misakiensis*, when HAT (GCN5) was inhibited with

Journal of Experimental Biology (2019) 222, jeb203620. doi:10.1242/jeb.203620

CPTH2 (cyclopentylidene [4′-(4-chlorophenyl)thiazol-2-yl] hydrazone). This suggests that *P. misakiensis* either has a built-in redundancy for the targeted HAT protein or that it is not essential for regeneration. However, CPTH2 exposure during budding, a mechanism of asexual reproduction in these species, caused downregulation of trans-differentiation-related genes (Shibuya et al., 2015), implying that HAT is important for asexual reproduction.

Together, regenerative studies looking at HDAC and other epigenetic modifiers demonstrate their importance in allowing appropriate re-establishment of the tissue by increasing cell proliferation and growth, followed by appropriate cell differentiation. Therefore, epigenetic processes are of interest to studying regenerative mechanisms in many species, but this has been largely unexplored in tunicate models such as *B. leachii*.

The current hypothesis is that either the cells lining the vascular vessels or circulating cells in a *B. leachii* colony act as the 'stem' cell population for WBR (Rinkevich et al., 2010). To allow the putative 'stem' cells in *B. leachii* to become activated and enter a proliferative state at the onset of WBR, the chromatin architecture likely needs to be modified to allow a rapid shift in gene expression to occur. Once activated, these cells move into the vascular lumen and are predicted to be the source of progenitors for many cell types of the new zooid during WBR (Rinkevich et al., 2010). We hypothesise that during WBR cell fate activation, differentiation and/or reprogramming of somatic cells occurs through chromatin modifications. To test this, we firstly identified *HDAC* and *HAT* genes in the *B. leachii* transcriptome (Zondag et al., 2016), and analysed their expression across regeneration stages. We found that *HDACI* and *HDACII* genes were expressed at high levels throughout WBR. Secondly, inhibition of HDACI/II activity by VPA halted the WBR process, and resulted in changes to the expression of key regeneration-related genes including *Piwi*, a gene used as a marker of stemness.

MATERIALS AND METHODS

Identification of *B. leachii* orthologues and phylogenetic analysis

Botrylloides leachii (Savigny 1816) orthologues of HAT, HDAC and histone proteins (Table S1) were identified using a TBLASTN 2.2.26+ against the entire *B. leachii* transcriptome using conserved protein domain sequences (Dataset 1). Contig identification was additionally confirmed by reciprocal BLAST using SMARTBLAST (https://blast.ncbi.nlm.nih.gov/smartblast/). Conserved protein domains used for identification of these domains in HAT/KAT proteins are listed in Table S2.

To assign subgroups to *B. leachii* HAT and HDAC orthologues, phylogenetic analysis was carried out with full-length sequences. Amino acid sequences were aligned with ClustalX (Jeanmougin et al., 1998), followed by Bayesian analysis using MrBayes (Ronquist et al., 2012) for 10,000 generations under a mixed model for HDAC proteins, and a fixed model (Jones) for HAT, both with a burn-in of 250. For expression analysis, RNA-seq count data (Zondag et al., 2016) were normalised to library size to determine expression changes across regeneration stages (Dataset 2).

Botrylloides leachii husbandry and regeneration

Botrylloides leachii colonies were collected from Otago Harbour (latitude 45.87°S, longitude 170.53°E) in New Zealand and cultured as described previously (Zondag et al., 2016).

Regeneration of *B. leachii* zooids from vascular fragments was carried out as previously published (Zondag et al., 2016). All zooids and buds from the marginal ampullae were removed using a fine tungsten needle. The vessel fragments attached to the slides were returned to the aerated seawater tanks and monitored under a Leica M205 FA stereomicroscope. Imaging was performed using the Leica DFC490 digital camera. Regenerating fragments were then removed from the glass slides for protein or RNA isolation.

Botrylloides leachii staging

Staging of regeneration stages was carried out as per Zondag et al. (2016); images are shown in Fig. S1. Briefly, stages were defined as follows: (A) *B. leachii* colony; (0) marginal ampullae at 0 h directly after dissection from the zooids has taken place; (1) new vascular connections formed between ampullae and terminal ampullae are still in initial cone-shape form; (2) marginal ampullae start to reshape and condense together; (3) remaining ampullae have completely condensed; (4) formation of small transparent vesicle in the middle of the condensed blood vessels, this transparent ball continues to expand and gain pigment before forming the new zooid; (5) a fully functioning zooid capable of filter feeding.

Chemical inhibition of HDAC activity

VPA was diluted in seawater to give a final concentration of 1 mmol l^{-1}. Dissected *B. leachii* colonies (leaving only vascular tissue) were submerged in aerated containers filled with 900 ml seawater containing either VPA or seawater only in the control. Seawater and VPA were replaced every other day. WBR was monitored for 18 days.

TSA was diluted in ethanol (EtOH) to a stock concentration of 4 mmol l^{-1}. *Botrylloides leachii* colonies were dissected (leaving only vascular tissue) and then submerged in aerated containers filled with filtered seawater containing either TSA at a final concentration of 50 nmol l^{-1}, or for the controls, the same volume of EtOH without TSA. Seawater and TSA/EtOH were replaced every other day; WBR was monitored for 18 days.

Regeneration score

WBR in *B. leachii* vascular fragments was scored after 18 days post regeneration induction through dissection of adults. Regeneration scoring was used as a way of quantifying regeneration success. The score reflected the regeneration stage the tunic tissue had reached after 18 days, and whether the vascular fragments looked healthy or were in the process of dying or were dead. The varied regeneration abilities were classed between 0 and 10. For example, if the vascular fragment was healthy and had regenerated to an adult, a regeneration score (RS) of 10 was given. However, if the tissue had died in the first stages (stages 1–2) of WBR, it was classed as a 0 (failed regeneration). Each of the regenerating tissue fragments was assigned an RS that was used to determine the effect of VPA on regeneration. A Mann–Whitney test was carried out comparing the VPA exposed fragments with the controls.

RT-qPCR analysis

RT-quantitative PCR (RT-qPCR) was carried out using total RNA extracted from VPA-exposed vascular tunic fragments or parallel-run controls. Both tissues were collected between 15 and 24 h post WBR induction. RNA extractions and cDNA synthesis (500 ng of total RNA) were performed as described previously (Zondag et al., 2016). All samples were assayed in triplicate with the SYBR Select Master Mix (ThermoFisher). The RT-qPCR reaction protocol consisted of 50°C for 2 min, 96°C for 2 min (40 cycles of 96°C for 15 s, 55–60°C for 30 s and 72°C for 1 min), followed by a dissociation curve program. RT-qPCR data were analysed with the ΔC_t (change in cycle threshold) method using $2^{-(\Delta C_t)}$ to determine

relative RNA expression to the reference genes, *Rpl27* and *Rsp29*. Gene expression fold change (FC) was calculated by determining the $\log_2$(VPA-treated/control) using relative expression levels. A list of RT-qPCR oligonucleotide sequences is provided in Table S3.

Measurement of nuclear acetyl-proteins

The Plant Nuclei Isolation/Extraction Kit (CelLyticPN, Sigma-Aldrich) was used to carry out the nuclear protein extractions. Tissues used for extraction were VPA-treated and control tissue undergoing WBR and both were collected at 15 h post adult dissection. Antibodies used for the dot blot were: primary antibody goat polyclonal anti-pan-Acetyl (Santa Cruz Biotechnology) (sc-8649) and secondary antibody donkey anti-goat-800 (LI-COR Biosciences; 925-32214).

Protein extracts were diluted in 1× SDS buffer [β-mercaptoethanol (0.1%), Bromophenol Blue (0.0005%), glycerol (10%), SDS (2%) in 63 mmol l^{-1} TrisCl, pH 6.8] to produce five 2-fold serial dilutions. One microlitre of diluted protein was placed onto a nitrocellulose membrane and left to dry for 30 min. Membranes were then soaked in REVERT (LI-COR Biosciences) stain for 5 min and washed twice with REVERT wash buffer prior to scanning at 700 nm. The membrane was then blocked in Odyssey blocking buffer for 30 min, followed by addition of the anti-pan-acetyl antibody (1 in 1000 in blocking buffer). Following an overnight incubation at 4°C with rocking, the membrane was washed three times with PBTw [PBS with Tween-20 (0.5%)] for 10 min each. The secondary antibody, anti-goat-800 (1 in 5000) was added and the membrane was left to incubate for 1 h at room temperature. The membrane was washed three times with PBTw, then a single wash with PBS, and left to dry before scanning at 800 nm. REVERT total protein stain (LI-COR Biosciences) was used for normalization of protein levels. Membranes were scanned using the Odyssey Imaging System. For protein quantification, signal intensity values were used to normalize anti-pan-acetyl antibody staining to total protein signal using the ImageStudioLite application (LI-COR Biosciences).

Histology

Control and VPA-treated fragments were fixed in 4% paraformaldehyde (PFA) for 1 h at room temperature. They were then removed from the glass slides and washed once in PBS before dehydration and embedding in paraffin, orientated for sagittal sections. Paraffin blocks were cut into 5-µm sections by the histology unit (University of Otago) and stained with haematoxylin and eosin (H&E). Stained sections were imaged with an Olympus AX70 light microscope.

Proliferating cell antigen (PCNA) staining

Botrylloides leachii sections were deparaffinized and rehydrated through an ethanol:water dilution series. Antigen retrieval was carried out with slides immersed in 10 mmol l^{-1} sodium citrate buffer (pH 6.0) and microwaved for 30 min. Slides were then rinsed with ddH_20 several times before continuing onto the immunohistochemistry protocol. Slides were then washed several times with PBTx (PBS plus 0.025% Triton X-100) for 5 min. Non-specific binding sites were blocked with PBS containing 1% BSA for 2 h. PCNA primary mouse monoclonal conjugated to horseradish peroxidase (Santa Cruz, sc-56-HRP) was diluted to a concentration of 1 in 500 in blocking buffer. Following an overnight incubation at 4°C, slides were washed three times with PBTx. Staining was carried out using the Invitrogen DAB plus kit according to the manufacturer's instructions. The colour reaction was stopped by washing the slides with ddH_20 and slides were mounted for imaging with an Olympus AX70 microscope (40× objective).

In situ hybridisation

Primers were designed to amply specific gene fragments from *B. leachii* cDNA (Table S3). PCR products were then cloned into pCRII-TOPO (Life Technologies) and sequenced to confirm the correct insertion of the product. Dioxygenin (DIG)-labelled sense and anti-sense RNA probes were synthesised using 10× DIG RNA labelling mix and SP6/T7 RNA polymerases (Sigma-Aldrich) in *in vitro* transcription reactions.

Different stages of regenerating *B. leachii* fragments were fixed in 4% PFA and dehydrated in 70% methanol, embedded in paraffin and sectioned to 5 µm. Hybridisation of probes to tissue sections was performed using Breitschopf et al.'s (1992) method for paraffin-embedded tissues with the following changes. Briefly, sections were rehydrated through a xylene–ethanol series into PBS, fixed with 4% PFA and incubated with proteinase K (2 µg ml^{-1} in PBS) for 10 min, followed by re-fixing with 4% PFA for 10 min. Following three washes with PBS, slides were acetylated and then incubated with hybridisation buffer for 1 h. DIG-labelled probes were added to hybridisation solution [50% formamide, 5× saline sodium citrate buffer (SSC), 0.1% Triton X-100, 0.5% CHAPS] and slides were incubated overnight at 60°C.

Following washing with 5× SSC and 0.2× SSC at room temperature, slides were blocked with TNB buffer (50 mmol l^{-1} TrisCl, pH 7.5, 150 mmol l^{-1} NaCl with 10% sheep serum) for 1 h before incubation with anti-DIG conjugated with alkaline phosphatase (Roche), diluted 1 in 2000 in TNB buffer overnight at 4°C. Slides were washed three times in TN buffer (50 mmol l^{-1} TrisCl, pH 7.5, 150 mmol l^{-1} NaCl) and finally with NTM buffer (10 mmol l^{-1} TrisCl, pH 9.5, 50 mmol l^{-1} $MgCl_2$, 0.1 mol l^{-1} NaCl). The colour reaction solution contained NBT/BCIP in NTM. Once sufficiently stained, slides were washed briefly in PBS plus 1% Triton X-100, fixed with 4% PFA, mounted with DAPI/glycerol and imaged with an Olympus AX70 light microscope. Cell types were identified based on appearance as previously published (Blanchoud et al., 2017; Table S4). When these were not clearly distinguishable, we classed them either as immunocytes (amoebocytes, morula and macrophage-like cells) or differentiating cells (transitionary cells, large nucleus, with an increased cytoplasm compared with the haemoblast cell).

RESULTS

Identification and classification of *B. leachii HDAC* and *HAT* genes

To initially determine whether HDAC and HAT enzymes are expressed during WBR, we identified transcripts for candidate orthologues within the regeneration transcriptome (Zondag et al., 2016) and further confirmed their identities using phylogenetics. For phylogenetic analysis, we included protein sequences from additional ascidians with sequenced genomes, one representing a solidary ascidian *Ciona robusta*, along with *Halocynthia roretzi*, *Molgula oculata* and *Botryllus schlosseri*, representing additional stolidobranchians. Candidate sequences from the *B. leachii* regeneration transcriptome and the *B. schlosseri* genome were identified by tBLASTn using conserved HAT and HDAC protein domains (Dataset 1) and confirmed by reciprocal BLAST.

There are four main classes of HDACs. Class I contains HDAC1, 2, 3 and 8; Class II contains HDAC 4, 5, 6, 7, 9 and 10; Class III includes the unrelated sirtuin (SIRT) family (NAD-dependent enzymes); and Class IV contains HDAC 11 (Gregoretti et al., 2004) (Fig. 1, Table S1). The classical HDAC proteins are considered to

Journal of Experimental Biology (2019) 222, jeb203620. doi:10.1242/jeb.203620

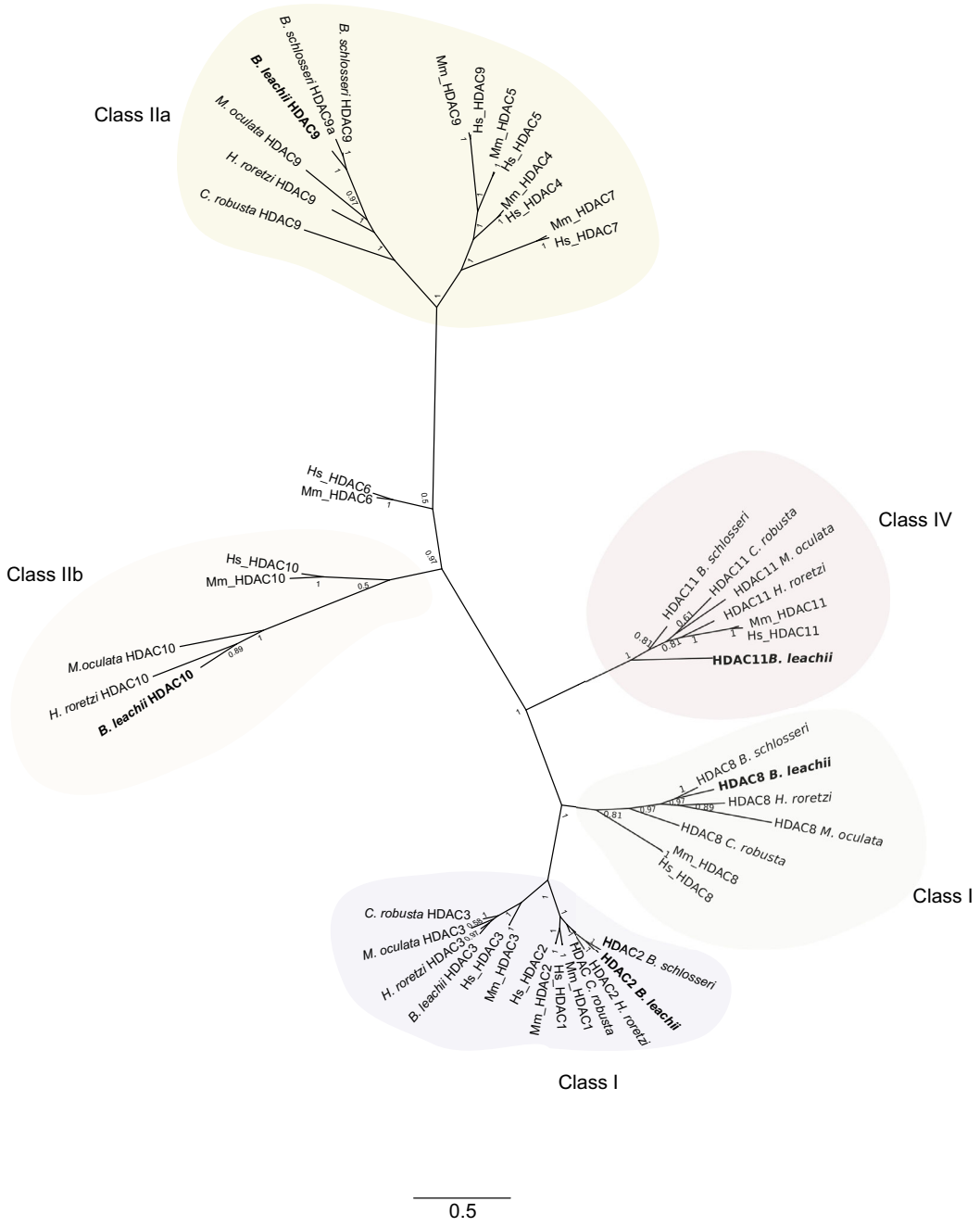

Fig. 1. Classification of *Botrylloides leachii* histone deacetylase (*HDAC*) and histone acetyltransferase (*HAT*) genes. Bayesian phylogeny for HDAC proteins displayed with FigTree (Ronquist et al., 2012). Sequences identified from *B. leachii* regeneration transcriptome, along with additional HDAC sequences from *Botryllus schlosseri*, *Molgula oculata*, *Halocynthia roretzi* and *Ciona robusta*, were used to construct the molecular phylogenetic tree to classify *B. leachii* HDAC proteins. Class I, II and IV all refer to the different HDAC classes. Hs, *Homo sapiens*; Mm, *Mus musculus*. Node labels are posterior probabilities.

have descended from a common ancestor (Gregoretti et al., 2004). We identified a total of six candidate transcripts expressed during WBR that encode HDAC-type proteins (Table S1). Phylogenetic analysis clustered these into separate clades, with representative sequences from mouse, human and ascidian genomes. We identified three *B. leachii* Class I type HDAC proteins (named Bl_HDAC3, Bl_HDAC8 and Bl_HDAC2). All three are also present in *C. robusta*, *H. roretzi* and *M. oculata* genomes, and two within the *B. schlosseri* genome (Bs_HDAC2 and Bs_HDAC8; Fig. 1). The class I HDAC proteins clustered tightly together, supporting a high level of sequence conservation for these proteins.

Class II proteins HDAC4/5/7/9 and HDAC6/10 are subclassified into Class IIa and ClassIIb, respectively (Fig. 1; Gregoretti et al., 2004). Two *B. leachii* HDAC proteins were classified as Class II HDACs: HDAC9 (IIa) and HDAC10 (IIb; Fig. 1). HDAC10 and HDAC5/9 proteins formed distinct groupings, suggesting more sequence divergence between Class II HDAC proteins. HDAC4–7 are found only in the vertebrates, and are thought to have arisen by gene duplication after the divergence of vertebrates and invertebrates (Gregoretti et al., 2004). Supporting this hypothesis, only a single copy of each Class IIa and IIb protein was found in ascidian genomes, with the exception of *B. schlosseri*, which has a

duplication of HDAC9 (Fig. 1). Lastly, a single Class IV protein, HDAC11, was identified in *B. leachii* and other ascidian genomes (Fig. 1).

HAT/KAT proteins are divided into subgroups through differences in sequence homology and function (Liew et al., 2013). Major HAT protein families include the MYST, GCN5-related proteins (GNAT) and the p300 family (Sapountzi and Côté, 2011). A total of seven HAT-related transcripts were identified in a BLAST search of the *B. leachii* transcriptome (Fig. 2, Table S1). As each HAT protein can have distinct cellular functions, we carried out phylogenetic analysis to classify into subgroups, along with vertebrates and four ascidians closely related to *B. leachii*.

Phylogeny analysis showed that within the *B. leachii* WBR transcriptome, orthologues for five MYST genes (*KAT2*, *KAT5*, *KAT6*, *KAT7* and *KAT8*), a single *p300* gene (*Bl_p300*) and a single GNAT gene (*Bl_HAT1*), are present. The KAT/HAT proteins separate into seven distinct groups with a single representative from each ascidian genome (Fig. 2A). Within most clades, the ascidian sequences clustered separately from the vertebrate group, suggesting that they are more closely related (Fig. 2A). In addition to the catalytic domain, HAT/KAT proteins contain further protein domains important for mediating molecular functions, and impart some specificity in KAT recruitment to particular chromatin sites, often termed 'reader' domains (Yun et al., 2011). As these additional protein domains are important for function, we identified KAT reader domains for *B. leachii* proteins (Fig. 2B, Table S3). Bl_HAT1 is the smallest KAT protein with no identifiable addition reader domains. HAT1 is often referred to a Type B histone acetyltransferase, an enzyme that acetylates free histone proteins before assembly into nucleosomes, with Type A histone acetyltransferases associated with chromatin binding (Parthun, 2007). Both Bl_p300 and Bl_KAT2 contain bromodomains; this region is important for the assembly of protein complexes and recognition of acetyl lysine (Dhalluin et al., 1999). Bl_KAT8 and Bl_KAT5 have tudor-knot domains; these mediate chromodomain interactions with RNA (Shimojo et al., 2008). We predict that Bl_KAT7 is likely to be a cytoplasmic protein owing to the presence of the FERM domain (Chishti et al., 1998; Fig. 2A).

Botrylloides leachii HDAC and *HAT* genes are consistently expressed during WBR

We next analysed the expression levels of each *HAT* and *HDAC* gene during WBR both in our previous RNA-seq data sets (Dataset 2; Zondag et al., 2016), and by RT-qPCR for highly expressed transcripts of further interest (Fig. 3).

HDAC transcripts showed some variation in expression levels across WBR and even between biological replicates (Fig. 3A). *Bl-HDAC2* (HDAC Class I) was expressed at higher levels than the other *HDAC* class genes (Dataset 2; >100 FPKM). Expression of *Bl-HDAC2* significantly increased between stages 0 and 3 (P=0.02, P_{adj}=0.01, one-way ANOVA, Tukey's multiple comparisons test), before declining again just prior to the appearance of the new zooid between stages 3 and 5 (Fig. 3A; P=0.04). *Bl-HDAC9* mRNA levels remained at a similar level across all examined time points (Fig. 3A). The *B. leachii* HDAC Class IV gene (*Bl_HDAC11*) was expressed at similar levels across all regeneration stages (Fig. 3A).

All seven *HAT* genes were expressed at varying levels during WBR (Dataset 2; Fig. 3B); we confirmed expression for the top four genes by RT-qPCR. *Bl_p300* transcript expression remained at similar levels through the first four stages of WBR, before a slight increase between stages 4 and 5 (~96–168 h; Fig. 3B). *Bl_HAT1* expression declined during the first 15 h of WBR (Fig. 3B). *Bl-KAT7* mRNA expression was maintained at a similar expression level across WBR (Fig. 3B, Dataset 2). *Bl_KAT8* expression increases between stages 1 and 3, to peak at stage 3 (P=0.02; Fig. 3B) before declining back to expression levels similar to those of earlier stages at stage 5 (P=0.04; Fig. 3B). *Bl_KAT6*, *Bl_HAT2A* and *Bl_KAT5* were expressed at much lower levels throughout WBR (<10 FPKM; Dataset 2).

HDAC inhibition halts *B. leachii* WBR

HDAC enzymes of Class I and II had the highest transcript levels in the HDAC family (Fig. 3A). To determine whether HDACI/II function is required for successful WBR, we used an HDAC chemical inhibitor. VPA is an established inhibitor of HDAC Class I/IIa (Gottlicher et al., 2001). It blocks HDAC activity by displacing the zinc ion interacting with the catalytic site of HDAC (de Ruijter et al., 2003). Therefore, successful HDAC inhibition would be expected to increase acetylation levels of cellular proteins. We confirmed that VPA treatment increased total acetylation levels for nuclear proteins using an antibody raised against acetyl-peptides (anti-pan-acetyl). The total amount of acetylated protein increased by ~2.5-fold (Fig. S2).

Although new zooids were normally observed by day 10, HDAC inhibitor experiments were performed for a total of 18 days to allow a definite conclusion as to the final stage of WBR. The majority (69%) of VPA-treated vascular fragments died during stages 3 and 4 (Fig. 4A). Only one of the regenerating fragments developed past stage 4 (siphons in the developing zooid had started to emerge). However, malformations were seen at stage 4 as the regeneration niche was merging with surrounding tissue (Fig. 4B), and between stages 4 and 5, where abnormal siphons and darkening of the fragment indicated it was not healthy, and this fragment subsequently died (Fig. 4B).

To further examine the effect of HDAC inhibition with VPA, regenerating fragments were collected at 48 h and 5 days post zooid removal for histology (Fig. 5). Typically, by 48 h, regenerating vascular fragments have reached stage 3, and regeneration niches have formed, often containing a bud (Fig. 5Ai–iii). However, in VPA-treated fragments, areas where ampullae have fused either had a bud that appeared abnormal (Fig. 5iv,v), or did not contain evidence of a regeneration bud anywhere in the vascular fragment (Fig. 5Avi,vii). Within control regenerating fragments left for 5 days, the regenerating bud zooid had formed the rudiments of branchial chamber and gut chambers (Fig. 5Bi,ii). In day 5 VPA-treated fragments that did form a regeneration bud, the latter failed to develop further, and appeared to be either degenerating or had not formed at one end (asterisks in Fig. 5Biii,iv).

Finally, to additionally confirm that HDAC activity was needed for successful regeneration, we used a second known HDAC inhibitor, TSA. Seven out of eight TSA-treated fragments stopped regeneration during stages 3–4 of the regeneration process and subsequently died during the remaining 15 days of the experiment. Although one fragment survived the length of the experiment (18 days), it had only reached stage 4 (Fig. S5). Control fragments (n=8) showed a better regeneration response with five fragments fully regenerating to stage 5 (fully functional adult). Three fragments that were in the process of regenerating began to look unhealthy by day 8 and appeared to have died by 18 days (Fig. S3). This could be partly due to the addition of ethanol to the seawater. Ethanol was used to dilute the TSA; thus, the same volume of ethanol was added to the controls. The results of the TSA

Journal of Experimental Biology (2019) 222, jeb203620. doi:10.1242/jeb.203620

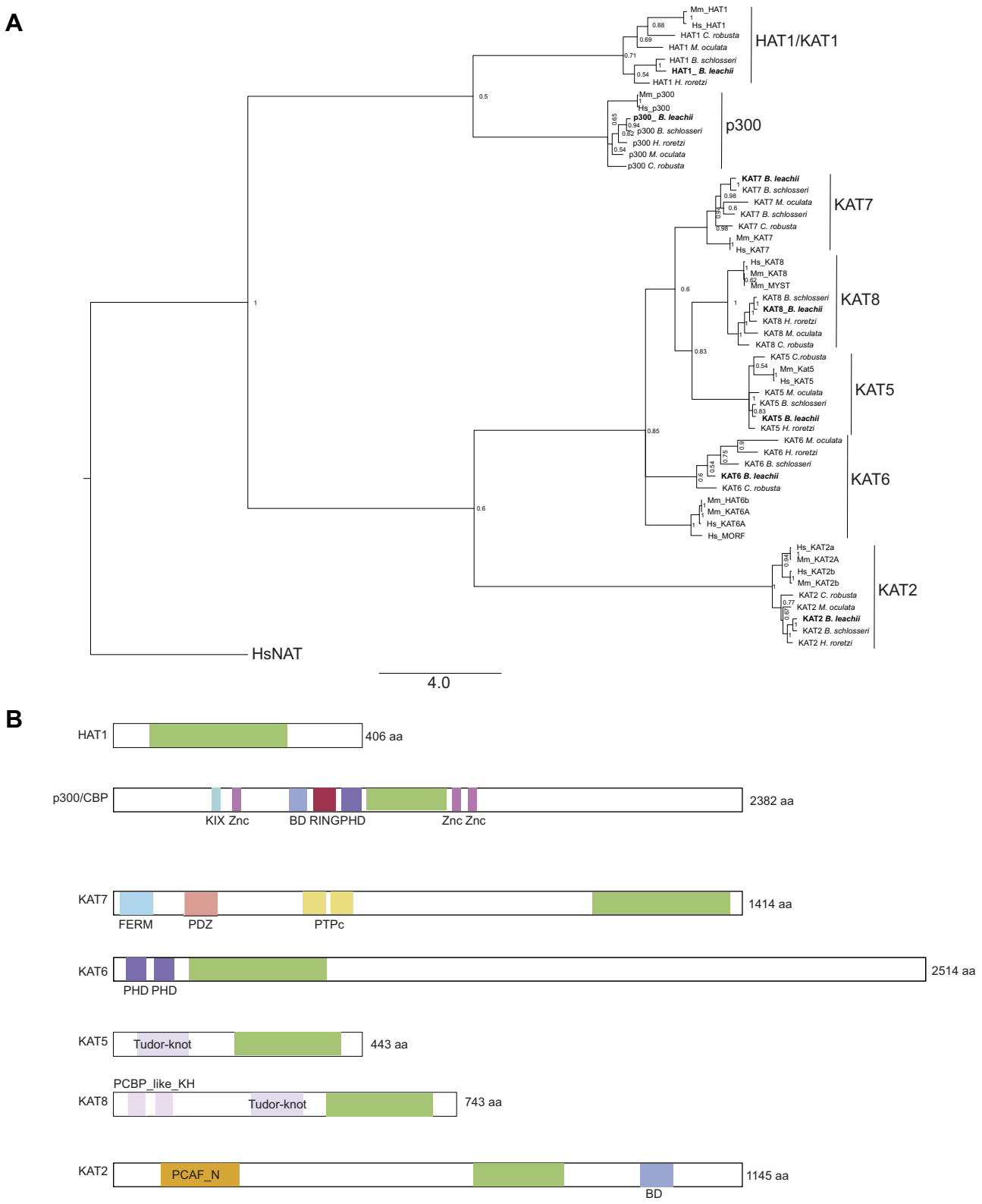

Fig. 2. Classification of *B. leachii HAT*/*KAT* genes. Identified *B. leachii HAT*/*KAT* genes were classified through phylogeny and the identification of additional protein domains. (A) Bayesian phylogeny for HAT proteins displayed with FigTree (Ronquist et al., 2012) with additional HAT sequences from *B. schlosseri*, *M. oculata*, *H. roretzi* and *C. robusta*. HsNAT (N-acetyltransferase) was used to root the tree. Node labels are posterior probabilities. (B) Protein domains present in *B. leachii* KAT proteins. The acetyltransferase catalytic domain (green) is flanked by additional protein domains important for conferring functional specificity to each KAT/HAT protein. Hs, *Homo sapiens*; Mm, *M. musculus*; BD, Bromodomain; PHD, Plant HomeoDomain; Znc, Zinc binding domain; FERM, 4.1 protein, ezrin, radixin, moesin; RING, Really Interesting New Gene; PCBP_like_KH, PolyC Binding Protein hnRNP K Homology; PCAF_N, p300/CBP-associated Factor N-terminal.

Journal of Experimental Biology (2019) 222, jeb203620. doi:10.1242/jeb.203620

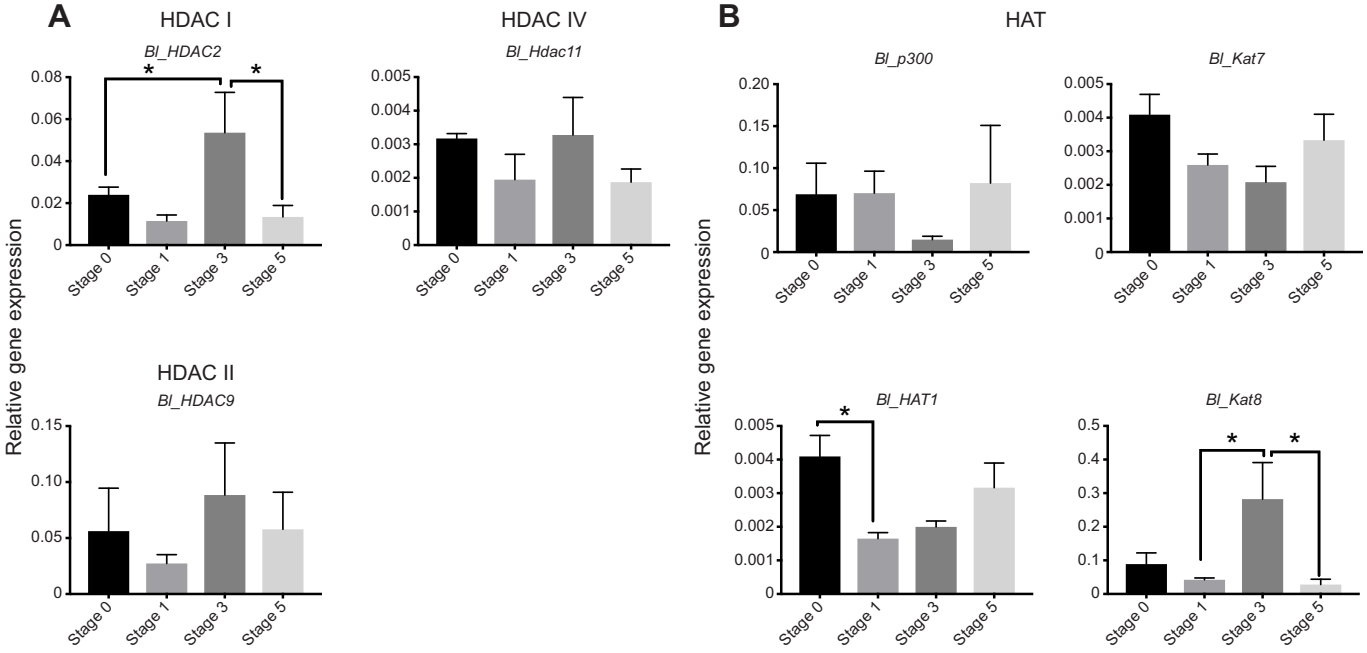

Fig. 3. *Botrylloides leachii HDAC* and *HAT* mRNA levels during whole-body regeneration (WBR). Relative expression levels for *HDAC* (A) and *HAT* (B) transcripts across three WBR stages following zooid removal. (A) WBR expression shown for the HDAC IV-type gene, *Bl_HDAC11*; HDAC II class gene, *Bl_HDAC2*; and HDAC III class gene, *Bl_HDAC9*. (B) Expression levels for *HAT* genes: *Bl_p300*, *Bl_HAT1*, *Bl_Kat8* and *Bl_Kat7*. Data are shown as means ±s.e.m. Statistical analysis was carried out using a one-way ANOVA, with Tukey's multiple comparison correction (*P<0.05).

experiment further supported the conclusions of the VPA-treatment experiments (Fig. 4), showing that HDAC activity is essential for successful WBR.

VPA treatment alters regeneration mRNA expression

To analyse the effect of reducing HDAC activity on mRNA levels, the expression of key regeneration genes (Zondag et al., 2016) was analysed in *B. leachii* fragments exposed to VPA in comparison to control fragments during regeneration (Fig. 6A). These genes were chosen as they were either differentially expressed between early regeneration stages (Zondag et al., 2016), or they have been previously linked to WBR in *B. leachii* (Rinkevich et al., 2008, 2010). RNA was extracted between stages 1 and 2 (~15–24 h) of WBR, as this was the stage that all VPA fragments were still healthy (Fig. 4).

The enzyme nitric oxide synthase (NOS) produces nitric oxide, a small molecular regulator of many biological processes, including tissue regeneration (Jaszczak et al., 2015; Rai et al., 1998). Previously, we found that *Bl_NOS* mRNA expression increased ~3-fold during early WBR (Transcript ID: comp16908, P_{adj}<0.05; Zondag et al., 2016). HDACi decreased *Bl_NOS* levels by 2.7-fold (P=0.02), compared with control fragments (Fig. 6A).

Slit genes encode proteins important for axon guidance during development but are also reactivated during axon regeneration in planarians (Cebrià et al., 2007). *Botrylloides leachii Slit2* mRNA is expressed by circulatory cells within early stage regeneration niches (Rinkevich et al., 2008) and its expression increases between early and mid-WBR (P_{adj}<0.05; Fig. S4). Regeneration in the presence of VPA reduced *Bl_Slit2* transcription by 2.2-fold (P<0.001; Fig. 6A).

Bl_TGF-β mRNA was upregulated significantly 3-fold during early WBR (stages 0–2; Fig. S4; Zondag et al., 2016). In contrast, inhibition of HDAC activity by VPA significantly reduced expression of *Bl_TGF-β* (P=0.03; Fig. 6A). Components of both canonical and non-canonical Wnt signalling were downregulated and upregulated, respectively, between early and late stages of WBR (Zondag et al., 2016). Expression of the Wnt receptor *Bl_Frizzed-4* (*Bl_Fzd4*) declined during early WBR and significantly increases between stages 3 and 5 (P_{adj}=0.02; Fig. S4). HDACi resulted in a ~2-fold reduction of *Bl_Fzd4* mRNA (P=0.04; Fig. 6A), suggesting that HDAC activity is required for *Bl_Fzd4* expression.

Bl_ColX1 (*comp17500*) is predicted to encode a fibrillar collagen isoform X1 protein (ColX1). Previously, we found that transcription of *Bl_ColX1* significantly declined during the first 24 h of WBR (P_{adj}<0.05; Zondag et al., 2016). Treatment with VPA resulted in a further reduction of *Bl_ColX1* mRNA compared with matched control samples (P=0.01, unpaired two-tailed *t*-test; Fig. 6A). This suggests that reduced HDAC activity leads to a further suppression of *Bl_ColX1* gene expression.

Bl_Tm-like (*comp2742*) is predicted to encode a metalloproteinase (MMP) with thrombospondin motifs (Zondag et al., 2016). MMPs are required for remodelling of the extracellular matrix (ECM) during regeneration in vertebrates (Bai et al., 2005; Vinarsky et al., 2005). *Bl_Tm-like* transcript expression declined 3-fold following induction of WBR (Zondag et al., 2016). Fragments regenerating in the presence of VPA further increased transcript levels by almost 2-fold compared with control regenerating fragments (P=0.03; Fig. 6A).

PCNA has been used as a marker of cell proliferation during *B. leachii* WBR (Rinkevich et al., 2007). Circulating haemocytes stain with PCNA during the earliest phase of regeneration, and, at 2 days post regeneration induction, PCNA staining was observed in cell aggregates within regeneration niches (Rinkevich et al., 2007). HDAC activity promotes cell cycle progression and cell proliferation in some cell types and can directly interact with PCNA (Bhaskara et al., 2013; Glozak and Seto, 2007; Milutinovic et al., 2002). Thus, we determined whether *PCNA* mRNA expression was affected by treatment with VPA. *Bl_PCNA*

Journal of Experimental Biology (2019) 222, jeb203620. doi:10.1242/jeb.203620

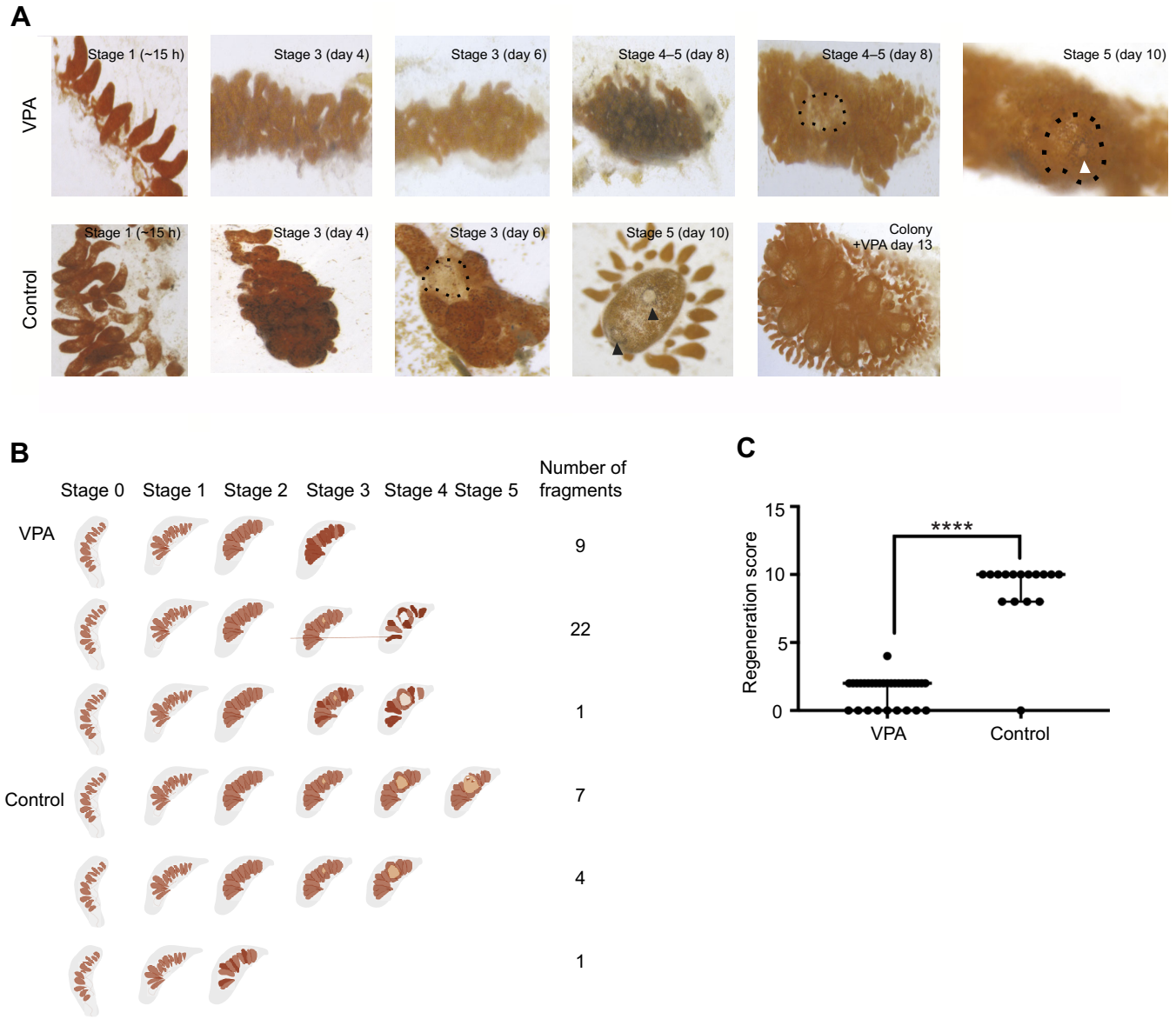

Fig. 4. HDAC inhibition prevents completion of WBR. *Botrylloides leachii* vascular tissue exposed to valproic acid (VPA) showed successful progression of WBR until stage 3. (A) Example images of regenerating tunicate fragments in the presence of VPA. Most fragments showed signs of death (darkening and covered in a white film) around days 4–6. One *B. leachii* vascular fragment exposed to VPA reached stage 4, as a regeneration niche is visible (dotted outline); however, a malformed siphon started to develop (stage 5, white arrowhead) before the regenerating tissue started to darken and died. Control fragments showed a typical WBR process, with a regeneration niche (dotted outline) forming around days 5–6 and a zooid at day 10 (black arrowheads indicate siphons). Intact colonies exposed to VPA for the same length of time were healthy. (B) Summary of the stages during WBR that vascular fragments exposed to VPA (or control) reached after 18 days of culturing, along with number of fragments that reached each stage. (C) Regeneration scores of HDACi experiments after leaving the vascular fragments for a total of 18 days. There was a significant difference (Mann–Whitney test $P<0.0001$) between regeneration score results of the VPA exposed fragments versus the controls. Data show medians±interquartile range. ****$P\leq0.0001$.

mRNA levels decreased 1.6-fold with VPA treatment ($P=0.03$; Fig. 6A), suggesting that HDAC activity was needed for correct *PCNA* transcription during WBR. To further investigate this, we stained regenerating fragments with antibodies against PCNA (Fig. 6B). Control fragments showed strong staining for PCNA in cell aggregates and regenerating buds (Fig. 6B). PCNA staining of VPA-treated fragments showed reduced antibody staining (Fig. 6B), further suggesting reduced levels of PCNA protein.

Piwi genes encode RNA-binding proteins, expressed in both the germ line and adult pluripotent stem cells (van Wolfswinkel, 2014). The *Bl_Piwi* gene plays a key role in WBR; its expression increases during WBR, initially in cells that line the blood vessel epithelium and later in cells throughout the vessel lumen (Rinkevich et al., 2010). *Bl_Piwi* gene knockdown arrests regeneration, and these fragments lack regeneration buds and cell aggregates (Rinkevich et al., 2010). We found that HDACi leads to increased expression of *Bl_Piwi*, in comparison with control fragments ($P=0.008$; Fig. 6A), suggesting dysregulation of *Bl_Piwi* gene expression. *In situ* hybridisation for *Bl_Piwi* in control fragments found that it was highly expressed in haemoblasts and some immunocytes (Fig. 7A,B). *Bl_Piwi* mRNA was also still detectable in some transitioning (or differentiating) cells; these cells have a larger cytoplasm compared with haemoblasts (Fig. 7B, arrows; Blanchoud et al., 2017). Following exposure to VPA, *Bl_Piwi* mRNA was found in

Journal of Experimental Biology (2019) 222, jeb203620. doi:10.1242/jeb.203620

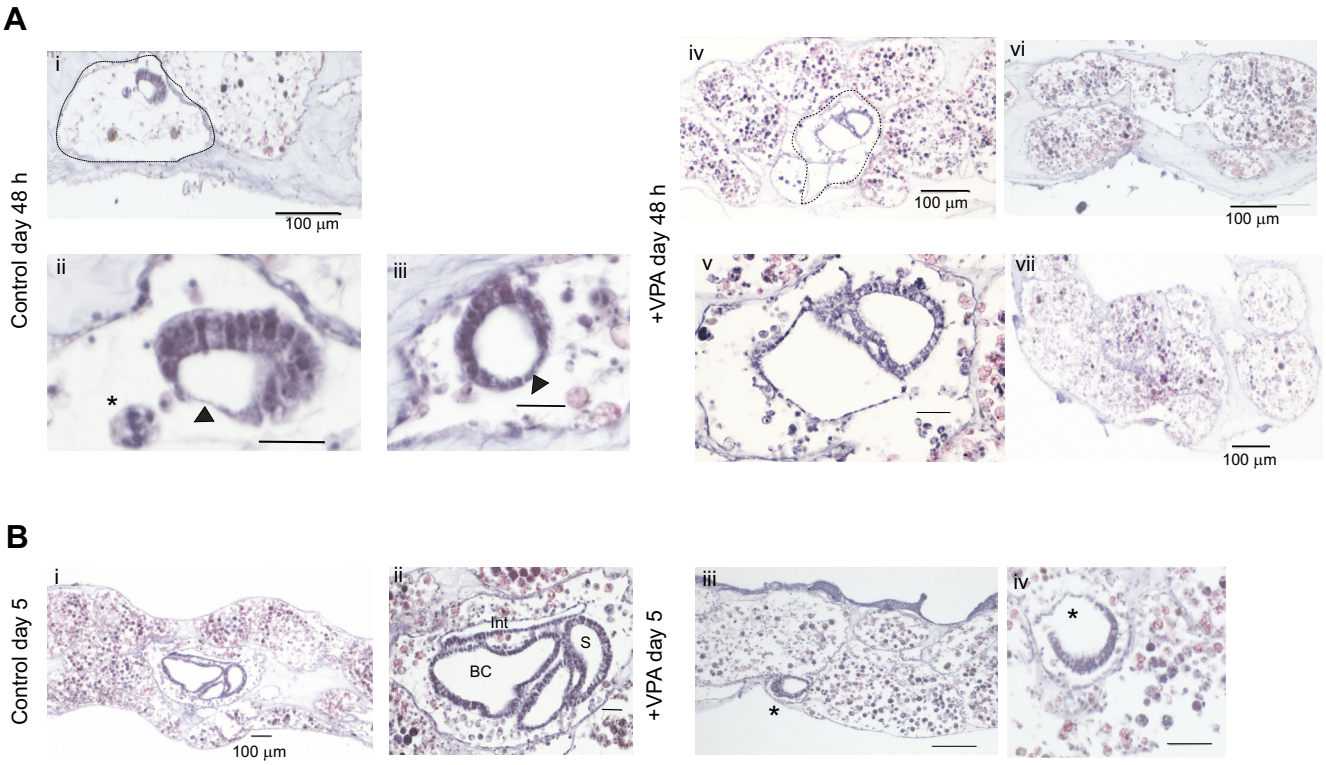

Fig. 5. Histology of control and VPA-treated fragments. (A) Control (i–iii) and VPA-treated (iv–vii) fragments collected at 48 h. At this stage of regeneration, control fragments have formed regeneration niches (dashed line, i and iv), containing an epithelial bud that is thinning on one side (ii and iii, arrowhead). Often, a cell aggregate (ii, asterisk) is observed nearby (depending upon the level of section through the fragment). Most VPA-treated fragments fail to form a regeneration bud at 48 h (vi and vii), and those that contain a bud appear to be malformed (iv and v; higher magnification). (B) By day 5, control fragments have a regenerating zooid, with rudiment tissue layers forming (i and ii), whereas VPA-treated fragments either contain no buds or a degenerating malformed bud (iii and iv, asterisk). Scale bars indicate 25 µm unless otherwise indicated. BC, branchial chamber; S, stomach; Int, intestine.

additional cell types throughout the haemolymph (Fig. 7C), including macrophage-like cells and cell aggregates (Fig. 7D).

In control fragments, *Bl_NOS* mRNA was detected in immunocytes, cell aggregates and haemoblasts, and the regeneration bud epithelium (Fig. 7E,F). *Bl_NOS* mRNA expression, which decreased with HDACi (Fig. 6A), was also more difficult to detect by *in situ* hybridisation following VPA treatment (Fig. 7G,H). In the VPA-treated fragments, *Bl_NOS* was only detectable in haemoblasts and some amoebocytes (Fig. 7F).

HDAC2, *HDAC9* and *Kat8* genes are expressed in most cell types during WBR

As WBR is halted mid-way through by HDACi, resulting in dysregulation of gene expression, we determined the corresponding spatial expression of *Bl_HDAC2* and *Bl_Kat8* mRNA at mid-WBR (stage 3; Fig. 8). *Bl_HDAC2* mRNA was expressed largely by morula cells in *B. leachii* circulation at stage 3 and by some transitioning cells (Fig. 8A). Cell aggregates and the regenerating bud did not express *Bl_HDAC2* (Fig. 8A).

Bl_HDAC9 mRNA was detected more widely, in most immunocyte cell types (Fig. 8B). It was also expressed by cells that appeared to be differentiating cells and haemoblast cells (Fig. 8B). *Bl_HDAC9* mRNA was found in epithelial cells, located at one end of the regeneration bud and in some nearby cell aggregates (Fig. 8B, asterisks). *Bl_Kat8* was also expressed broadly in amebocytes, differentiating cells and haemoblasts (Fig. 8C). The regeneration bud also showed higher expression in one area of the epithelium (Fig. 8C; asterisks) and some cell aggregates surrounding the developing bud (Fig. 8C; dashed circle), but was absent from others (Fig. 8C; arrowheads).

DISCUSSION

Identification and expression of HDAC and HAT genes during WBR

Examination of the *B. leachii* genome alongside additional ascidian genomes revealed that each ascidian genome had two Class I, two Class II and a single Class IV *HDAC* gene. This is also true for other invertebrates such as *Drosophila*, providing further evidence that the metazoan ancestor genome contained two Class I, two Class II and a single Class IV *HDAC* gene, and that the increase in vertebrate *HDAC* gene numbers is due to gene duplication (Gregoretti et al., 2004). The ascidian genomes examined contained a single representative for each HAT/KAT subclass.

HDAC and HAT function in regulating chromatin structural changes and DNA accessibility to globally control transcription from the genome. Two important aspects that restrict function of these proteins are their overall availability (expression level) and their enzymatic activity (Haberland et al., 2009; Legube and Trouche, 2003). As such, we focused on *HAT* and *HDAC* genes highly expressed during WBR, assuming this indicates that they have important roles in this process. Although RNA analysis does not factor in post-translational changes such as phosphorylation, known to alter enzymatic activity (Legube and Trouche, 2003), any dynamic changes to mRNA expression levels are likely to have a functional consequence for genome expression during regeneration. The differences in expression levels between family members is

Journal of Experimental Biology (2019) 222, jeb203620. doi:10.1242/jeb.203620

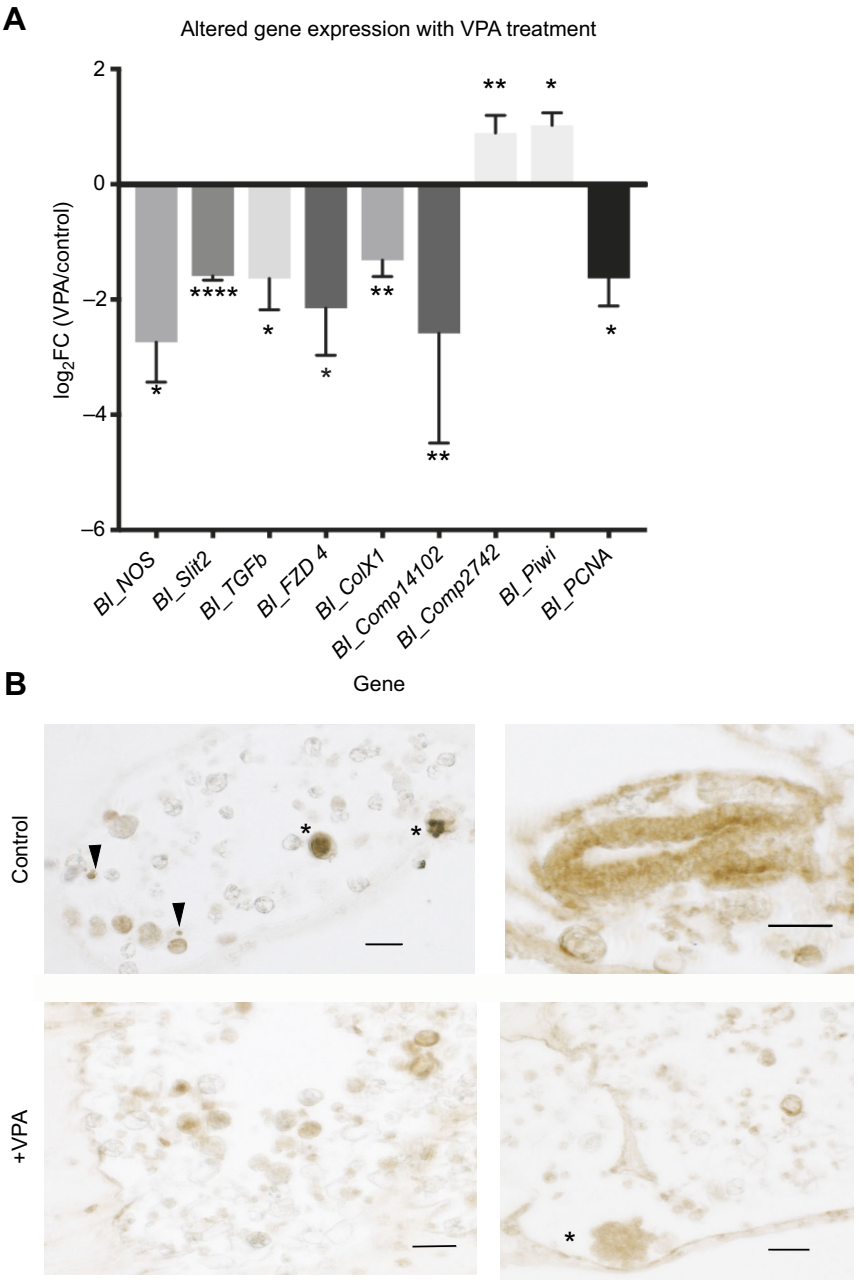

Fig. 6. Altered gene and proliferating cell antigen (PCNA) expression upon inhibition of HDACI/II activity. RT-qPCR and immunostaining for PCNA revealed molecular changes upon HDACi. (A) Fold change in transcription of *Bl_Fzd*, *Bl_NOS*, *Bl_Slit2*, *Bl_TGF-β*, *Bl_Piwi*, *Bl_PCNA*, *Bl_Tm-like* and *Bl_ColX1* in VPA-treated tissue undergoing WBR compared with matched controls. VPA-treated and control tissue were collected between 15 and 24 h after removal of all zooids. Data show means±s.e.m., unpaired two-tailed *t*-test (*P<0.05, **P<0.005, ****P<0.0001). (B) PCNA staining of control and VPA-treated fragments, collected at 48 h post zooid removal. In the controls, strong staining was detected in cell aggregates (asterisks) and small individual cells that resemble haemyoblast cells (arrowheads). Cells of the regenerating bud also stained strongly for PCNA (right panel). VPA-treated fragments (+VPA) showed weaker staining for PCNA overall, even within large cell aggregates (asterisk) and smaller differentiating cells (black arrowheads). Some positive staining was also observed for macrophage-like cells. Scale bars are 20 µm.

likely due to divergent cellular functions. Class I HDAC proteins are mostly confined to the cell nucleus (Delcuve et al., 2012; Seto and Yoshida, 2014), and are important for cell proliferation and differentiation (Reichert et al., 2012), whereas Class II HDAC proteins shuttle between the nucleus and the cytoplasm, and are thought to have more tissue-specific functions (Delcuve et al., 2012; Seto and Yoshida, 2014).

The expression of the *B. leachii* Class II HDAC, *Bl_HDAC2* mRNA, peaked at stage 3 (Fig. 3). During stage 3, regeneration niches appear containing epithelial buds that later form a new zooid. This is also the stage when HDACi stalls regeneration (Fig. 4). *Bl_HDAC2* expression in the circulating haemocytes is restricted to the immunocytes and morula cells, with weaker expression within the regeneration bud (Fig. 8). Notably, *B. leachii HDAC* genes were not expressed in all epithelial cells of the regenerating bud, but were enriched within cells located at the posterior end of the bud, across from the developing endostyle (Fig. 8). HDAC activity is required for axis patterning and cell lineage commitment in other animals (Brunmeir et al., 2009; Carneiro et al., 2011; Lv et al., 2014), suggesting that *B. leachii HDAC* genes may function in the development of specific tissue layers. This may additionally relate to the observation in HDACi histology sections that HDACi fragments with a bud present after 1 week exhibit one end poorly formed. However, it is not possible to distinguish whether one end had formed and the bud had halted development, or was in the process of degeneration (Fig. 5). HDAC1/2 complexes have important roles in differentiation of certain cell types and determining the fate of embryonic stem cells (ESCs) (Dovey et al., 2010; Turgeon et al., 2013; Ye et al., 2009). It is possible that HDACi resulted in a change of cell lineage commitment, promoting one cell fate over another, resulting in failure of the regeneration bud to continue development.

MYST/KAT genes are required for stem cells and developmental processes (Sapountzi and Côté, 2011). KAT8 (MYST1/MOF) proteins have multiple cellular roles including controlling cell cycle

Journal of Experimental Biology (2019) 222, jeb203620. doi:10.1242/jeb.203620

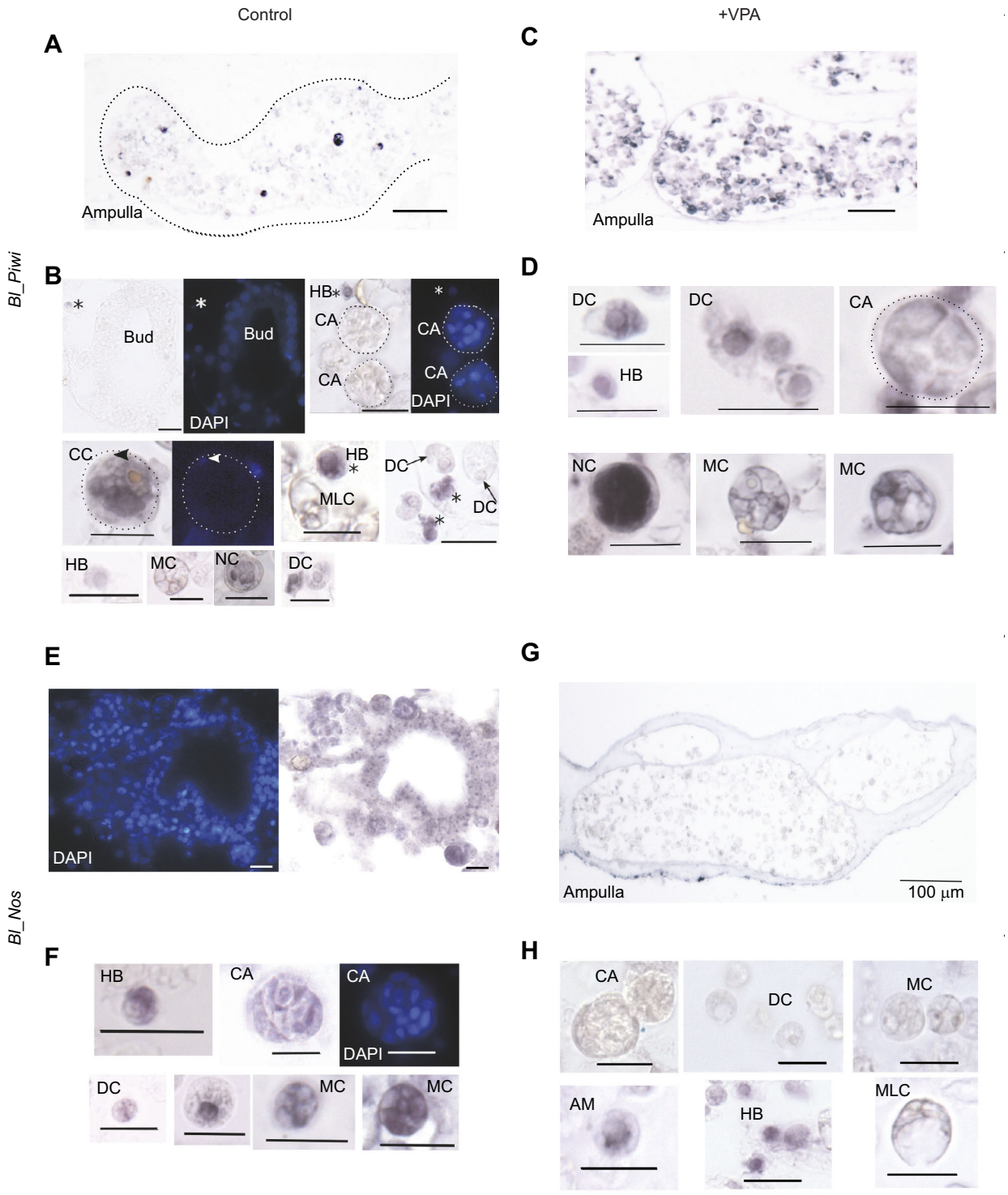

Fig. 7. Detection of *Bl_Piwi* and *Bl_NOS* mRNA following HDACi. *In situ* hybridisation for *Bl_Piwi* and *Bl_NOS* mRNA during WBR in control and VPA-treated fragments. DAPI images are shown for comparison. (A) Control WBR *Bl_Piwi* expression was detected in cells located in some of the condensed ampullae. (B) Higher-magnification images of Piwi-positive and -negative cells. Small cells expressing *Bl_Piwi* mRNA (asterisks) are haemoblasts. Cells with a higher cytoplasm to nucleus ratio (transitional or differentiating cells) also showed some positive staining (arrows). Some compartment cells were positive for *Bl_Piwi* mRNA (CC nucleus indicated by arrowhead). Weaker staining was detected in morula and nephrocytes. No staining was observed in the regenerating bud, cell aggregates and macrophage-like cells. (C) *Bl_Piwi* mRNA is detected in cells throughout the ampullae following VPA treatment during WBR. (D) Higher magnification images of cells expressing *Bl_Piwi* mRNA. These include haemoblast cells, cell aggregates and larger vacuole containing immunocytes, with a morphologies similar to macrophage and morula cell types (Table S3). (E,F) *Bl_NOS* mRNA was detected in haemoblasts and morula cells and cell aggregates (DAPI image showing multiple nuclei) as well as the epithelium of the regenerating bud (E). (G,H) VPA treatment reduced overall staining for *Bl_NOS* mRNA (ampullae shown in G), with some mRNA still detected in haemoblasts and amoebocytes (H) but is largely absent from other cell types include cell aggregates. HB, haemoblast; MC, morula cell; CA, cell aggregate; MLC, macrophage-like cell; DC, differentiating cell; AM, amoebocyte; NC, nephrocyte cell; CC, compartment cell. Scale bars are 10 µm, unless otherwise shown.

Journal of Experimental Biology (2019) 222, jeb203620. doi:10.1242/jeb.203620

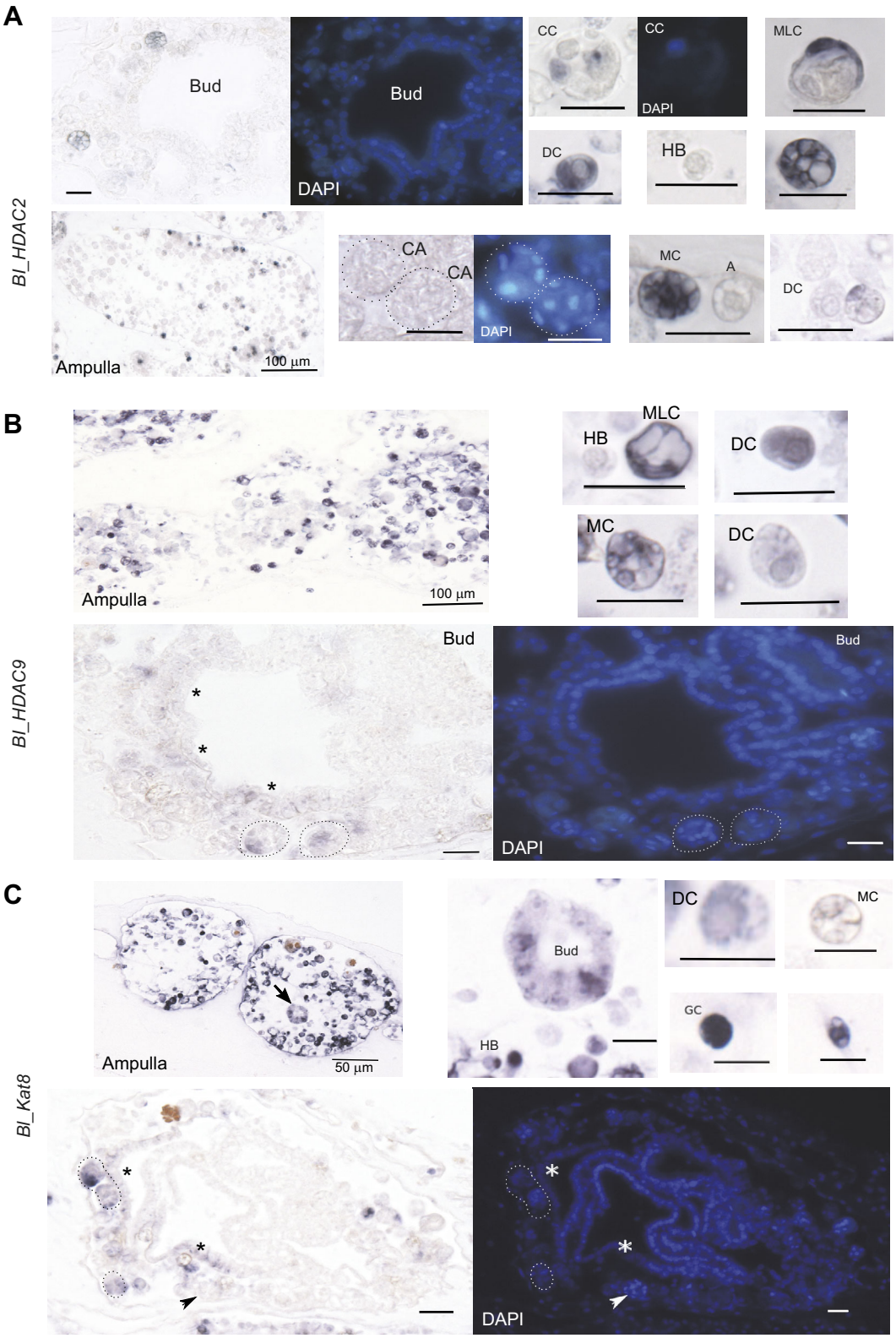

Fig. 8. Expression of *Bl_HDAC2*, *Bl_HDAC9* and *Bl_Kat8* in WBR fragments. *In situ* hybridisation was used to detect expression of target transcripts in sectioned WBR fragments collected two days after removal of all zooids. DAPI staining is also shown to aid identification. (A) *Bl_HDAC2* mRNA was detected in morula cells throughout the ampullae, but was absent from cell aggregates, haemoblasts, differentiating cells and the regeneration niche. (B) *Bl_HDAC9* mRNA was detected in most cell types including immunocytes such as morula cells, and haemoblasts. Cells of the regenerating bud, located at one end (asterisks), also expressed Bl_HDAC9 mRNA, along with some nearby cell aggregates (dashed lines). (C) Staining for *Bl_Kat8* mRNA was found in multiple circulating haemocytes including haemoblasts, small differentiating cells, cell aggregates, early bud and immunocytes. It was expressed by haemocytes located near the regeneration bud and by cells at one end of the bud (arrowheads). HB, haemoblast; MC, morula cell; CA, cell aggregate; IC, immunocyte; DC, differentiating cell; MLC, macrophage-like cell; am, amoebocyte. Scale bars are 10 µm, unless otherwise shown.

progression (Thomas et al., 2008), pluripotency and regulating expression of core ESC genes (Li et al., 2012). *Bl_KAT8* transcript levels peaked at stage 3 (Fig. 3), and were detected in immunocytes, haemoblasts and differentiating cells (Fig. 8).

Although the focus here is regeneration, it is likely that HDAC and HAT/KAT activity is also required for asexual reproduction in *B. leachii*. Later stages of WBR are likely to be similar to asexual reproduction, particularly following formation of a regeneration bud, which is morphologically similar to the blastogenesis budlet (Kürn et al., 2011). GCN5 (also called KAT2a) activity is required for blastogenesis in *P. misakiensis* but not zooid regeneration (Shibuya et al., 2015). We also note that *KAT2* expression is lower compared with that of other *HAT/KAT* genes, suggesting it may not have a key role in colonial ascidian regeneration. As there is functional redundancy between HAT/KAT proteins (Nugent et al., 2010), we predict that use of a broader HAT inhibitor would have also halted regeneration in *P. misakiensis*. However, in the future it would be of interest to use specific knockdown of each *KAT* gene to determine whether they have specific roles in asexual reproduction and regeneration.

Changes to mRNA expression during WBR resulting from HDACi

HDACi altered the expression of genes typically upregulated or downregulated during WBR, indicating that changes in transcription are likely to have played a role in failure of regeneration observed with VPA and TSA treatment. Although HDAC activity is more commonly associated with progressing chromatin into a more compressed heterochromatin structure, it can also cause an increase in transcription owing to suppression of repressor expression (Glaser et al., 2003). This suggests that the correct implementation of WBR-associated transcription patterns requires HDAC function and protein deacetylation.

Modification of the ECM is important for facilitating regeneration (Bonnans et al., 2014). HDACi did alter expression of these genes; their expression altered in a direction (up or down) similar to that of normal WBR. Additionally, given that HDACi did not halt condensation and reorganisation of the ampullae (Figs 3 and 4), this further suggests that HDAC activity and protein deacetylation does not play an essential role in the reorganisation of the vascular tissue during early WBR.

Cell proliferation is an important factor in regeneration, providing a source of cells for the generation of replacement tissues (Sanchez Alvarado and Tsonis, 2006). In our study, HDACi decreased PCNA levels as determined by both RT-qPCR and immunohistochemistry (Fig. 6). Previous studies investigating mouse liver and kidney regeneration also showed that HDAC function is required for increasing PCNA levels (Tang et al., 2014; Wang et al., 2008), indicating that this may be a feature not only of WBR, but also of many types of regenerative processes across different phyla.

Bl_Slit2 transcription typically increased between stages 0 to 3 of WBR. HDACi significantly reduced *Bl_Slit2* mRNA levels, indicating that HDAC activity is required for upregulation of *Bl_Slit2* gene expression. *Slit2* gene expression is directly regulated by HDAC5 (a Class II HDAC) in mammalian endothelial cells (Urbich et al., 2009). This gene may function in regulating the vascular rearrangements that occur during *B. leachii* WBR.

Bl_NOS transcription also reduced with HDACi treatment. NOS is essential for the generation of nitric oxide, which has important roles in pluripotency and immune responses (Beltran-Povea et al., 2015; Cencioni et al., 2018; Lee et al., 2017). *Bl_NOS* mRNA is expressed in multiple cell types including haemoblasts and the regeneration niche. Thus, its expression pattern during WBR suggests that nitric oxide also has important roles in these biological processes within *B. leachii* colonies. The reduction of NOS expression by HDACi could be due to loss of whole regeneration niches (that express *NOS*) and/or a reduction of certain *NOS*-positive cell types following HDACi treatment.

Hypothesis and model for HDACI/II function in *B. leachii* WBR

During *B. leachii* regeneration, a new bud forms that is located within a regeneration niche, beside an aggregate of stem-like/haemoblast cells that express the pluripotency gene *Piwi* (Fig. 7A). The acetylation and de-acetylation of nuclear proteins is important

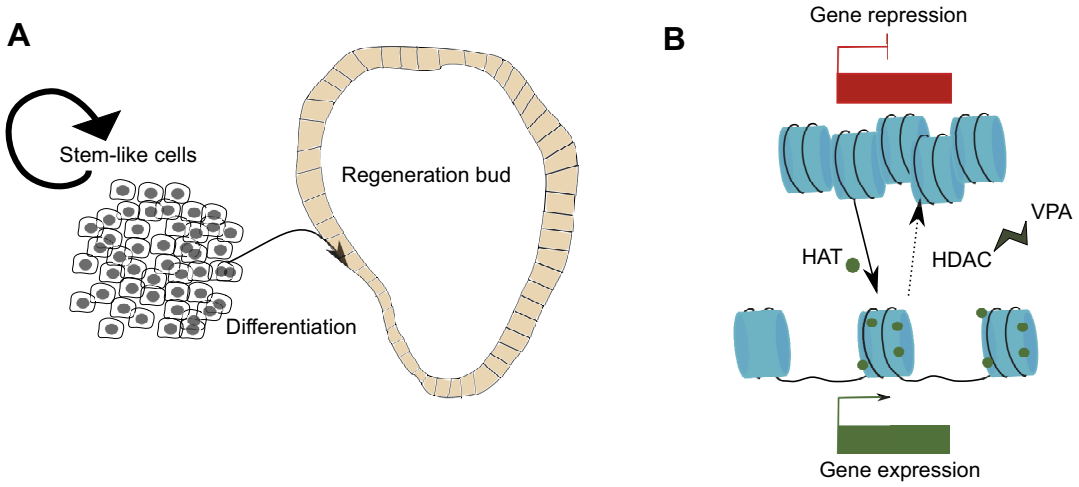

Fig. 9. Model of HDAC inhibition. Schema depicting a model for *B. leachii* WBR and histone acetylation by HDAC/HAT enzymes. (A) Hypothesis for *B. leachii* regeneration based on current and earlier studies (Rinkevich et al., 1995, 2010). WBR is initiated with an increase in stem-like cells (Piwi-positive cells) (Rinkevich et al., 2010). These form a cell aggregate inside a regeneration niche; an area where several ampullae have fused. Around stage 2–3, ~24–48 h post zooid removal, cells exit this aggregate and form an epithelial regeneration bud before differentiating into specialized cell types found in a mature zooid. (B) HAT and HDAC enzymes regulate gene expression from the *B. leachii* genome, compact (heterochromatin) and open forms of chromatin (euchromatin). HDAC inhibition (by VPA) increased acetylation of nuclear proteins, leading to halting of WBR and altered transcription of genes required for differentiation.

for correct transcription during development and regeneration (Huang et al., 2014; Taylor and Beck, 2012; Tseng et al., 2011). Thus, HDAC activity is required between stages 3 and 4, a critical period requiring changes to gene expression, promoting differentiation and tissue patterning, to generate a new zooid (Fig. 9). Previous examination of differential gene expression found that the levels of over 500 transcripts declined between stages 3 and 4 (Zondag et al., 2016; Fig. S5), compared with increased expression of only 39 genes; this potentially could be a result of histone de-acetylation and the expression of repressor proteins. Future studies will include RNA-seq (following HDACi), alongside chromatin immunoprecipitation experiments, for a more global approach to identifying targets of histone acetylation during WBR.

Given the importance of histone deacetylation in gene regulation and differentiation, it may be a conserved method utilised by many animals to regulate changes to global transcription from the genome during regeneration. Reduced HDAC activity also prevents formation of the blastema in the cnidarian *Hydractinia* head regeneration by both HDACi and HDAC2 knockdown (Flici and Frank, 2018; Flici et al., 2017). In vertebrates, HDACi prevents hindlimb muscle regeneration in mice (Spallotta et al., 2013), and tail and limb regeneration in *Xenopus* (Taylor and Beck, 2012; Tseng et al., 2011). Chemical inhibition of HDAC function in zebrafish does not interfere with the initial stages of fin regeneration (healing and blastema formation), but causes later defects, preventing differentiation of cells and reducing tail outgrowth (Pfefferli et al., 2014). We also found that HDACi did not block the initial stages of regeneration, instead stopping regeneration after the ampullae had condensed to form the regeneration niches, at the bud formation and differentiation stage. Therefore, although all of these animals use different modes of regeneration, such as blastema formation, cell dedifferentiation and stem cells to repair and replace lost tissue, they all require HDAC function for successful regeneration.

Conclusions

Inhibition of HDAC activity caused a dysregulation in transcription and ultimately led to a failure of the vascular tissue undergoing cellular differentiation during WBR. During the first 24 h of WBR, existing tissue is reorganised, including fusion of some ampullae, followed by formation of a regeneration niche at stage 3. HDACi alters transcription and halts regeneration at stage 3. Therefore, we predict that HDAC is needed to allow the putative 'stem' cells to undergo differentiation and/or to proliferate. Future work using the *B. leachii* genome (Blanchoud et al., 2018) and mapping of epigenetic marks will aid our understanding of how these epigenetic modifiers influence global gene expression.

Acknowledgements

We thank James Smith, Lyvianne Decourtye, Jeremy McCallum-Loudeac, Susie Szakats, Michael Meier and Stephanie Workman for feedback on earlier drafts of the paper.

Competing interests

The authors declare no competing or financial interests.

Author contributions

Formal analysis: L.Z.; Investigation: L.Z., R.M.C., M.J.W.; Resources: M.J.W.; Writing - original draft: L.Z., R.M.C., M.J.W.; Writing - review & editing: R.M.C., M.J.W.; Supervision: M.J.W.; Funding acquisition: M.J.W.

Funding

We would like to thank the School of Biomedical Sciences (Deans Bequest Grant), Department of Anatomy and the Royal Society of New Zealand Marsden fund (UOOO1713) for funding support. L.Z. was supported by a University of Otago PhD scholarship.

Supplementary information

Supplementary information available online at
http://jeb.biologists.org/lookup/doi/10.1242/jeb.203620.supplemental

References

Bai, S., Thummel, R., Godwin, A. R., Nagase, H., Itoh, Y., Li, L., Evans, R., McDermott, J., Seiki, M. and Sarras, M. P., Jr (2005). Matrix metalloproteinase expression and function during fin regeneration in zebrafish: analysis of MT1-MMP, MMP2 and TIMP2. *Matrix Biol.* **24**, 247-260. doi:10.1016/j.matbio.2005.03.007

Bannister, A. J. and Kouzarides, T. (2011). Regulation of chromatin by histone modifications. *Cell Res.* **21**, 381-395. doi:10.1038/cr.2011.22

Beltran-Povea, A., Caballano-Infantes, E., Salguero-Aranda, C., Martin, F., Soria, B., Bedoya, F. J., Tejedo, J. R. and Cahuana, G. M. (2015). Role of nitric oxide in the maintenance of pluripotency and regulation of the hypoxia response in stem cells. *World J. Stem. Cells* **7**, 605-617. doi:10.4252/wjsc.v7.i3.605

Bhaskara, S., Jacques, V., Rusche, J. R., Olson, E. N., Cairns, B. R. and Chandrasekharan, M. B. (2013). Histone deacetylases 1 and 2 maintain S-phase chromatin and DNA replication fork progression. *Epigenetics Chromatin* **6**, 27. doi:10.1186/1756-8935-6-27

Blanchoud, S., Zondag, L., Lamare, M. D. and Wilson, M. J. (2017). Hematological analysis of the ascidian *Botrylloides leachii* (Savigny, 1816) during whole-body regeneration. *Biol. Bull.* **232**, 143-157. doi:10.1086/692841

Blanchoud, S., Rutherford, K., Zondag, L., Gemmell, N. J. and Wilson, M. J. (2018). De novo draft assembly of the *Botrylloides leachii* genome provides further insight into tunicate evolution. *Sci. Rep.* **8**, 5518. doi:10.1038/s41598-018-23749-w

Bonnans, C., Chou, J. and Werb, Z. (2014). Remodelling the extracellular matrix in development and disease. *Nat. Rev. Mol. Cell Biol.* **15**, 786-801. doi:10.1038/nrm3904

Breitschopf, H., Suchanek, G., Gould, R. M., Colman, D. R. and Lassmann, H. (1992). In situ hybridization with digoxigenin-labeled probes: sensitive and reliable detection method applied to myelinating rat brain. *Acta Neuropathol.* **84**, 581-587. doi:10.1007/BF00227734

Brunmeir, R., Lagger, S. and Seiser, C. (2009). Histone deacetylase HDAC1/HDAC2-controlled embryonic development and cell differentiation. *Int. J. Dev. Biol.* **53**, 275-289. doi:10.1387/ijdb.082649rb

Carneiro, K., Donnet, C., Rejtar, T., Karger, B. L., Barisone, G. A., Diaz, E., Kortagere, S., Lemire, J. M. and Levin, M. (2011). Histone deacetylase activity is necessary for left-right patterning during vertebrate development. *BMC Dev. Biol.* **11**, 29. doi:10.1186/1471-213X-11-29

Cebrià, F., Guo, T., Jopek, J. and Newmark, P. A. (2007). Regeneration and maintenance of the planarian midline is regulated by a slit orthologue. *Dev. Biol.* **307**, 394-406. doi:10.1016/j.ydbio.2007.05.006

Cencioni, C., Spallotta, F., Savoia, M., Kuenne, C., Guenther, S., Re, A., Wingert, S., Rehage, M., Sürün, D., Siragusa, M. et al. (2018). Zeb1-Hdac2-eNOS circuitry identifies early cardiovascular precursors in naive mouse embryonic stem cells. *Nat. Commun.* **9**, 1281. doi:10.1038/s41467-018-03668-0

Chishti, A. H., Kim, A. C., Marfatia, S. M., Lutchman, M., Hanspal, M., Jindal, H., Liu, S.-C., Low, P. S., Rouleau, G. A., Mohandas, N. et al. (1998). The FERM domain: a unique module involved in the linkage of cytoplasmic proteins to the membrane. *Trends Biochem. Sci.* **23**, 281-282. doi:10.1016/S0968-0004(98)01237-7

Delcuve, G. P., Khan, D. H. and Davie, J. R. (2012). Roles of histone deacetylases in epigenetic regulation: emerging paradigms from studies with inhibitors. *Clin. Epigenetics* **4**, 5. doi:10.1186/1868-7083-4-5

de Ruijter, A. J., van Gennip, A. H., Caron, H. N., Kemp, S. and van Kuilenburg, A. B. (2003). Histone deacetylases (HDACs): characterization of the classical HDAC family. *Biochem. J.* **370**, 737-749. doi:10.1042/bj20021321

Dhalluin, C., Carlson, J. E., Zeng, L., He, C., Aggarwal, A. K. and Zhou, M.-M. (1999). Structure and ligand of a histone acetyltransferase bromodomain. *Nature* **399**, 491-496. doi:10.1038/20974

Dovey, O. M., Foster, C. T. and Cowley, S. M. (2010). Histone deacetylase 1 (HDAC1), but not HDAC2, controls embryonic stem cell differentiation. *Proc. Natl. Acad. Sci. USA* **107**, 8242-8247. doi:10.1073/pnas.1000478107

Eisenhoffer, G. T., Kang, H. and Sanchez Alvarado, A. (2008). Molecular analysis of stem cells and their descendants during cell turnover and regeneration in the planarian *Schmidtea mediterranea*. *Cell Stem Cell* **3**, 327-339. doi:10.1016/j.stem.2008.07.002

Flici, H. and Frank, U. (2018). Inhibition of SoxB2 or HDACs suppresses *Hydractinia* head regeneration by affecting blastema formation. *Commun. Integr. Biol.* **11**, 1-5. doi:10.1080/19420889.2018.1450032

Flici, H., Schnitzler, C. E., Millane, R. C., Govinden, G., Houlihan, A., Boomkamp, S. D., Shen, S., Baxevanis, A. D. and Frank, U. (2017). An evolutionarily conserved SoxB-Hdac2 crosstalk regulates neurogenesis in a cnidarian. *Cell Rep.* **18**, 1395-1409. doi:10.1016/j.celrep.2017.01.019

Gan, Q., Yoshida, T., McDonald, O. G. and Owens, G. K. (2007). Concise review: epigenetic mechanisms contribute to pluripotency and cell lineage determination of embryonic stem cells. *Stem Cells* **25**, 2-9. doi:10.1634/stemcells.2006-0383

Glaser, K. B., Staver, M. J., Waring, J. F., Stender, J., Ulrich, R. G. and Davidsen, S. K. (2003). Gene expression profiling of multiple histone deacetylase (HDAC)

inhibitors: defining a common gene set produced by HDAC inhibition in T24 and MDA carcinoma cell lines. *Mol. Cancer Ther.* **2**, 151-163.
Glozak, M. A. and Seto, E. (2007). Histone deacetylases and cancer. *Oncogene* **26**, 5420-5432. doi:10.1038/sj.onc.1210610
Gottlicher, M., Minucci, S., Zhu, P., Kramer, O. H., Schimpf, A., Giavara, S., Sleeman, J. P., Lo Coco, F., Nervi, C., Pelicci, P. G. et al. (2001). Valproic acid defines a novel class of HDAC inhibitors inducing differentiation of transformed cells. *EMBO J.* **20**, 6969-6978. doi:10.1093/emboj/20.24.6969
Gregoretti, I. V., Lee, Y.-M. and Goodson, H. V. (2004). Molecular evolution of the histone deacetylase family: functional implications of phylogenetic analysis. *J. Mol. Biol.* **338**, 17-31. doi:10.1016/j.jmb.2004.02.006
Haberland, M., Montgomery, R. L. and Olson, E. N. (2009). The many roles of histone deacetylases in development and physiology: implications for disease and therapy. *Nat. Rev. Genet.* **10**, 32-42. doi:10.1038/nrg2485
Huang, J., Barr, E. and Rudnick, D. A. (2013). Characterization of the regulation and function of zinc-dependent histone deacetylases during rodent liver regeneration. *Hepatology* **57**, 1742-1751. doi:10.1002/hep.26206
Huang, J., Schriefer, A. E., Yang, W., Cliften, P. F. and Rudnick, D. A. (2014). Identification of an epigenetic signature of early mouse liver regeneration that is disrupted by Zn-HDAC inhibition. *Epigenetics* **9**, 1521-1531. doi:10.4161/15592294.2014.983371
Jaszczak, J. S., Wolpe, J. B., Dao, A. Q. and Halme, A. (2015). Nitric oxide synthase regulates growth coordination during drosophila melanogaster imaginal disc regeneration. *Genetics* **200**, 1219-1228. doi:10.1534/genetics.115.178053
Jeanmougin, F., Thompson, J. D., Gouy, M., Higgins, D. G. and Gibson, T. J. (1998). Multiple sequence alignment with Clustal X. *Trends Biochem. Sci.* **23**, 403-405. doi:10.1016/S0968-0004(98)01285-7
Jopling, C., Boue, S. and Izpisua Belmonte, J. C. (2011). Dedifferentiation, transdifferentiation and reprogramming: three routes to regeneration. *Nat. Rev. Mol. Cell Biol.* **12**, 79-89. doi:10.1038/nrm3043
Ke, Q., Yang, R.-N., Ye, F., Wang, Y.-J., Wu, Q., Li, L. and Bu, H. (2012). Impairment of liver regeneration by the histone deacetylase inhibitor valproic acid in mice. *J. Zhejiang Univ. Sci. B* **13**, 695-706. doi:10.1631/jzus.B1100362
Kürn, U., Rendulic, S., Tiozzo, S. and Lauzon, R. J. (2011). Asexual propagation and regeneration in colonial ascidians. *Biol. Bull.* **221**, 43-61. doi:10.1086/BBLv221n1p43
Lee, K. K. and Workman, J. L. (2007). Histone acetyltransferase complexes: one size doesn't fit all. *Nat. Rev. Mol. Cell Biol.* **8**, 284-295. doi:10.1038/nrm2145
Lee, M., Rey, K., Besler, K., Wang, C. and Choy, J. (2017). Immunobiology of nitric oxide and regulation of inducible nitric oxide synthase. *Results Probl. Cell Differ.* **62**, 181-207. doi:10.1007/978-3-319-54090-0_8
Legube, G. and Trouche, D. (2003). Regulating histone acetyltransferases and deacetylases. *EMBO Rep.* **4**, 944-947. doi:10.1038/sj.embor.embor941
Li, X., Li, L., Pandey, R., Byun, J. S., Gardner, K., Qin, Z. and Dou, Y. (2012). The histone acetyltransferase MOF is a key regulator of the embryonic stem cell core transcriptional network. *Cell Stem Cell* **11**, 163-178. doi:10.1016/j.stem.2012.04.023
Liew, L. C., Singh, M. B. and Bhalla, P. L. (2013). An RNA-seq transcriptome analysis of histone modifiers and RNA silencing genes in soybean during floral initiation process. *PLoS ONE* **8**, e77502. doi:10.1371/journal.pone.0077502
Lv, W., Guo, X., Wang, G., Xu, Y. and Kang, J. (2014). Histone deacetylase 1 and 3 regulate the mesodermal lineage commitment of mouse embryonic stem cells. *PLoS ONE* **9**, e113262. doi:10.1371/journal.pone.0113262
Marmorstein, R. and Roth, S. Y. (2001). Histone acetyltransferases: function, structure, and catalysis. *Curr. Opin. Genet. Dev.* **11**, 155-161. doi:10.1016/S0959-437X(00)00173-8
Milutinovic, S., Zhuang, Q. and Szyf, M. (2002). Proliferating cell nuclear antigen associates with histone deacetylase activity, integrating DNA replication and chromatin modification. *J. Biol. Chem.* **277**, 20974-20978. doi:10.1074/jbc.M202504200
Murakami, Y. (2013). Histone deacetylases govern heterochromatin in every phase. *EMBO J.* **32**, 2301-2303. doi:10.1038/emboj.2013.154
Nugent, R. L., Johnsson, A., Fleharty, B., Gogol, M., Xue-Franzen, Y., Seidel, C., Wright, A. P. and Forsburg, S. L. (2010). Expression profiling of S. pombe acetyltransferase mutants identifies redundant pathways of gene regulation. *BMC Genomics* **11**, 59. doi:10.1186/1471-2164-11-59
Parthun, M. R. (2007). Hat1: the emerging cellular roles of a type B histone acetyltransferase. *Oncogene* **26**, 5319-5328. doi:10.1038/sj.onc.1210602
Pfefferli, C., Müller, F., Jaźwińska, A. and Wicky, C. (2014). Specific NuRD components are required for fin regeneration in zebrafish. *BMC Biol.* **12**, 30. doi:10.1186/1741-7007-12-30
Rai, R. M., Lee, F. Y. J., Rosen, A., Yang, S. Q., Lin, H. Z., Koteish, A., Liew, F. Y., Zaragoza, C., Lowenstein, C. and Diehl, A. M. (1998). Impaired liver regeneration in inducible nitric oxide synthasedeficient mice. *Proc. Natl. Acad. Sci. USA* **95**, 13829-13834. doi:10.1073/pnas.95.23.13829
Reddien, P. W., Bermange, A. L., Murfitt, K. J., Jennings, J. R. and Sánchez Alvarado, A. (2005). Identification of genes needed for regeneration, stem cell function, and tissue homeostasis by systematic gene perturbation in planaria. *Dev. Cell* **8**, 635-649. doi:10.1016/j.devcel.2005.02.014
Reichert, N., Choukrallah, M.-A. and Matthias, P. (2012). Multiple roles of class I HDACs in proliferation, differentiation, and development. *Cell. Mol. Life Sci.* **69**, 2173-2187. doi:10.1007/s00018-012-0921-9
Rinkevich, B., Shlemberg, Z. and Fishelson, L. (1995). Whole-body protochordate regeneration from totipotent blood cells. *Proc. Natl. Acad. Sci. USA* **92**, 7695-7699. doi:10.1073/pnas.92.17.7695
Rinkevich, Y., Paz, G., Rinkevich, B. and Reshef, R. (2007). Systemic bud induction and retinoic acid signaling underlie whole body regeneration in the urochordate *Botrylloides leachi*. *PLoS Biol.* **5**, e71. doi:10.1371/journal.pbio.0050071
Rinkevich, Y., Rinkevich, B. and Reshef, R. (2008). Cell signaling and transcription factor genes expressed during whole body regeneration in a colonial chordate. *BMC Dev. Biol.* **8**, 100. doi:10.1186/1471-213X-8-100
Rinkevich, Y., Rosner, A., Rabinowitz, C., Lapidot, Z., Moiseeva, E. and Rinkevich, B. (2010). Piwi positive cells that line the vasculature epithelium, underlie whole body regeneration in a basal chordate. *Dev. Biol.* **345**, 94-104. doi:10.1016/j.ydbio.2010.05.500
Robb, S. M. C. and Sanchez Alvarado, A. (2014). Histone modifications and regeneration in the planarian *Schmidtea mediterranea*. *Curr. Top. Dev. Biol.* **108**, 71-93. doi:10.1016/B978-0-12-391498-9.00004-8
Ronquist, F., Teslenko, M., van der Mark, P., Ayres, D. L., Darling, A., Höhna, S., Larget, B., Liu, L., Suchard, M. A. and Huelsenbeck, J. P. (2012). MrBayes 3.2: efficient Bayesian phylogenetic inference and model choice across a large model space. *Syst. Biol.* **61**, 539-542. doi:10.1093/sysbio/sys029
Sanchez Alvarado, A. and Tsonis, P. A. (2006). Bridging the regeneration gap: genetic insights from diverse animal models. *Nat. Rev. Genet.* **7**, 873-884. doi:10.1038/nrg1923
Sapountzi, V. and Côté, J. (2011). MYST-family histone acetyltransferases: beyond chromatin. *Cell. Mol. Life Sci.* **68**, 1147-1156. doi:10.1007/s00018-010-0599-9
Seto, E. and Yoshida, M. (2014). Erasers of histone acetylation: the histone deacetylase enzymes. *Cold Spring Harb. Perspect Biol.* **6**, a018713. doi:10.1101/cshperspect.a018713
Shibuya, M., Hatano, M. and Kawamura, K. (2015). Interactive histone acetylation and methylation in regulating transdifferentiation-related genes during tunicate budding and regeneration. *Dev. Dyn.* **244**, 10-20. doi:10.1002/dvdy.24212
Shimojo, H., Sano, N., Moriwaki, Y., Okuda, M., Horikoshi, M. and Nishimura, Y. (2008). Novel structural and functional mode of a knot essential for RNA binding activity of the Esa1 presumed chromodomain. *J. Mol. Biol.* **378**, 987-1001. doi:10.1016/j.jmb.2008.03.021
Spallotta, F., Tardivo, S., Nanni, S., Rosati, J. D., Straino, S., Mai, A., Vecellio, M., Valente, S., Capogrossi, M. C., Farsetti, A. et al. (2013). Detrimental effect of class-selective histone deacetylase inhibitors during tissue regeneration following hindlimb ischemia. *J. Biol. Chem.* **288**, 22915-22929. doi:10.1074/jbc.M113.484337
Tang, J., Yan, Y., Zhao, T. C., Gong, R., Bayliss, G., Yan, H. and Zhuang, S. (2014). Class I HDAC activity is required for renal protection and regeneration after acute kidney injury. *Am. J. Physiol. Renal. Physiol.* **307**, F303-F316. doi:10.1152/ajprenal.00102.2014
Taylor, A. J. and Beck, C. W. (2012). Histone deacetylases are required for amphibian tail and limb regeneration but not development. *Mech. Dev.* **129**, 208-218. doi:10.1016/j.mod.2012.08.001
Thomas, T., Dixon, M. P., Kueh, A. J. and Voss, A. K. (2008). Mof (MYST1 or KAT8) is essential for progression of embryonic development past the blastocyst stage and required for normal chromatin architecture. *Mol. Cell. Biol.* **28**, 5093-5105. doi:10.1128/MCB.02202-07
Tseng, A.-S., Carneiro, K., Lemire, J. M. and Levin, M. (2011). HDAC activity is required during *Xenopus* tail regeneration. *PLoS ONE* **6**, e26382. doi:10.1371/journal.pone.0026382
Turgeon, N., Blais, M., Gagné, J.-M., Tardif, V., Boudreau, F., Perreault, N. and Asselin, C. (2013). HDAC1 and HDAC2 restrain the intestinal inflammatory response by regulating intestinal epithelial cell differentiation. *PLoS ONE* **8**, e73785. doi:10.1371/journal.pone.0073785
Urbich, C., Rossig, L., Kaluza, D., Potente, M., Boeckel, J.-N., Knau, A., Diehl, F., Geng, J.-G., Hofmann, W.-K., Zeiher, A. M. et al. (2009). HDAC5 is a repressor of angiogenesis and determines the angiogenic gene expression pattern of endothelial cells. *Blood* **113**, 5669-5679. doi:10.1182/blood-2009-01-196485
van Wolfswinkel, J. C. (2014). Piwi and potency: PIWI proteins in animal stem cells and regeneration. *Integr. Comp. Biol.* **54**, 700-713. doi:10.1093/icb/icu084
Vinarsky, V., Atkinson, D. L., Stevenson, T. J., Keating, M. T. and Odelberg, S. J. (2005). Normal newt limb regeneration requires matrix metalloproteinase function. *Dev. Biol.* **279**, 86-98. doi:10.1016/j.ydbio.2004.12.003
Wang, G.-L., Salisbury, E., Shi, X., Timchenko, L., Medrano, E. E. and Timchenko, N. A. (2008). HDAC1 promotes liver proliferation in young mice via interactions with C/EBPbeta. *J. Biol. Chem.* **283**, 26179-26187. doi:10.1074/jbc.M803545200
Ye, F., Chen, Y., Hoang, T., Montgomery, R. L., Zhao, X.-H., Bu, H., Hu, T., Taketo, M. M., van Es, J. H., Clevers, H. et al. (2009). HDAC1 and HDAC2 regulate oligodendrocyte differentiation by disrupting the β-catenin–TCF interaction. *Nat. Neurosci.* **12**, 829. doi:10.1038/nn.2333
Yun, M., Wu, J., Workman, J. L. and Li, B. (2011). Readers of histone modifications. *Cell Res.* **21**, 564-578. doi:10.1038/cr.2011.42
Zondag, L. E., Rutherford, K., Gemmell, N. J. and Wilson, M. J. (2016). Uncovering the pathways underlying whole body regeneration in a chordate model, Botrylloides leachi using de novo transcriptome analysis. *BMC Genomics* **17**, 114. doi:10.1186/s12864-016-2435-6